



Full length article

## Synthesis and characterization of citrate-based fluorescent small molecules and biodegradable polymers



Zhiwei Xie<sup>a</sup>, Jimin P. Kim<sup>a</sup>, Qing Cai<sup>b</sup>, Yi Zhang<sup>c</sup>, Jinshan Guo<sup>a</sup>, Ranjodh S. Dhama<sup>a</sup>, Li Li<sup>d</sup>, Bin Kong<sup>e</sup>, Yixue Su<sup>a</sup>, Kevin A. Schug<sup>d</sup>, Jian Yang<sup>a,\*</sup>

<sup>a</sup> Department of Biomedical Engineering, Materials Research Institutes, The Huck Institutes of Life Sciences, The Pennsylvania State University, University Park, PA 16801, United States

<sup>b</sup> Beijing Laboratory of Biomedical Materials, Beijing University of Chemical Technology, Beijing 100029, China

<sup>c</sup> Institute of Medical Engineering and Science, Massachusetts Institute of Technology, Cambridge, MA 02139, United States

<sup>d</sup> Department of Chemistry and Biochemistry, University of Texas at Arlington, Arlington, TX 76010, United States

<sup>e</sup> Institute of Chemistry, Chinese Academy of Sciences, Beijing 100190, China

### ARTICLE INFO

#### Article history:

Received 7 September 2016

Received in revised form 16 December 2016

Accepted 5 January 2017

Available online 6 January 2017

#### Keywords:

Fluorescence

Fluorescence spectroscopy

Dyes

Polymers

Degradable

### ABSTRACT

Novel citric acid based photoluminescent dyes and biodegradable polymers are synthesized via a facile “one-pot” reaction. A comprehensive understanding of the fluorescence mechanisms of the resulting citric acid-based fluorophores is reported. Two distinct types of fluorophores are identified: a thiozopolyridine family with high quantum yield, long lifetime, and exceptional photostability, and a dioxopyridine family with relatively lower quantum yield, multiple lifetimes, and solvent-dependent band shifting behavior. Applications in molecular labeling and cell imaging were demonstrated. The above discoveries contribute to the field of fluorescence chemistry and have laid a solid foundation for further development of new fluorophores and materials that show promise in a diversity of fluorescence-based applications.

#### Statement of Significance

Photoluminescent materials are pivotal for fluorescence based imaging, labeling and sensing applications. Understanding their fluorescence mechanism is challenging and imperative. We develop a new class of citric acid-derived fluorescent materials in forms of polymers and small molecular dyes by a one-step solvent free reaction. We discovered two different classes of citric acid-derived fluorophores. A two-ring thiozopolyridine structure demonstrates strong fluorescence and exceptional resistance to photobleaching. A one-ring dioxopyridine exhibits relative weak fluorescence but with intriguing excitation and solvent-dependent emission wavelength shifting. Our methodology of synthesizing citric acid-derived fluorophores and the understanding on their luminescence are instrumental to the design and production of a large number of new photoluminescent materials for biological and biomedical applications.

© 2017 Acta Materialia Inc. Published by Elsevier Ltd. All rights reserved.

### 1. Introduction

Fluorescence imaging is a powerful and versatile tool for applications ranging from molecular biology to disease diagnostics due to its high resolution and sensitivity. Advances in fluorescent imaging probes and technologies have empowered researchers to visualize and analyze biological systems in an unprecedented fashion [1,2]. Organic dyes are the most widely used and studied imaging agents, partly because their fluorescence mechanisms are well

understood. Several non-traditional fluorescent probes, including quantum dots, green fluorescent proteins, graphene oxides, and carbon dots have recently been developed. However, challenges still remain for both organic dyes and non-traditional light emitting probes. For example, poor photostability and short lifetimes of fluorescence proteins and organic dyes hinder their applications in continuous cellular imaging and lifetime imaging [3]. The *in vivo* applications of carbon dots, graphene oxides, and quantum dots are limited due to their intrinsic toxicities. These challenges present an urgent need of developing biocompatible fluorophores that have long lifetimes, excellent photostability, and suitable physical

\* Corresponding author.

E-mail address: [jxy30@psu.edu](mailto:jxy30@psu.edu) (J. Yang).

properties for a wide range of fluorescence imaging applications [4].

Recently, many efforts have been put into creating new organic fluorescent materials that meet these key challenges for biological and medical applications. For example, hyperbranching poly (amido amine) (PAMAM) dendrimers and citric acid-derived carbon dots have been used as novel imaging agents [5,6]. Despite their practical utility, the fluorescence mechanism of these non-traditional fluorescent materials remains unclear. For new fluorescence probes, it is important to understand their fluorescence mechanisms to further innovations. For example, the field of quantum dots was significantly boosted after the discovery that the fluorescence of quantum dots (QDs) is attributed to the energy band gap and size-dependent confinement [4].

Herein, we develop a novel family of water-soluble fluorescent dyes, referred to as citric acid-derived photoluminescent dyes (CPDs) through facile one-pot, organic solvent free reactions between citric acid and various primary amines such as amino acids. Two different classes of CPD are identified and their photoluminescent (PL) mechanisms are studied systematically by using time resolved fluorescence spectroscopy and computational modeling. We also investigated the “band-shifting behaviors” of these fluorophores for the first time. Parallels between the chemical structures and band-shifting behaviors of Biodegradable Photoluminescent Polymers (BPLPs) with those of PAMAM dendrimers and carbon dots may provide insight into the fluorescence mechanisms of these novel classes of fluorophores.

## 2. Experimental section

### 2.1. Synthesis of polymers and dyes

All chemicals and solvents were purchased from Sigma Aldrich (St. Luis, MO). Citric acid-derived photoluminescent dyes (CPDs) were synthesized by dissolving 50 mM citric acid (or tricarballic acid, succinic acid) and 50 mM of a primary amine or amino acid into 20 mL of DI water in a flask. The reaction was conducted at 140 °C, open cap, until water mostly evaporated, followed by applying vacuum for 4 h. Afterwards, the reaction was terminated by adding 25 mL cold DI water to dissolve the products. The thiazolo pyridine carboxylic acid (TPA) products were purified three times by recrystallization in DI water, and the dioxo-pyridine ring (DPR) products were purified by preparative HPLC with a Shimadzu HPLC system equipped with a C18 column and a fraction collector. The average yields for CA-Cys and CA-Ala were 34% and 28.9% respectively. Biodegradable photoluminescent polymers (BPLPs) were synthesized according to our previous method [7]. Briefly, 100 mM citric acid (or tricarballic acid, succinic acid), 100 mM 1,8-octanediol, and 20 mM of a primary amine or amino acid were reacted in a flask at 140 °C under nitrogen flow for 2 h. Next, 50 mL 1, 4-dioxane was added to terminate the reaction and dissolve the resulting polymer, followed by precipitation in DI water and lyophilization for purification. The average yields for BPLP-Cys and BPLP-Ala were 89.4% and 59.8%. All chemicals were purchased from Sigma-Aldrich and used without further purification.

### 2.2. Fluorescence of polymers and dyes

Fluorescence spectra were recorded on a Horiba FluoroMax-4 spectrofluorometer (Horiba Scientific, Edison NJ). All CPDs were dissolved in DI water at optical density <0.1, and fluorescence measured with excitation and emission slit sizes of 1 nm by 1 nm unless otherwise specified. The fluorescence properties of polymers were measured in 2 wt% 1,4-dioxane solutions under same

settings as above. BPLPs were hydrolyzed in 1 M K<sub>2</sub>CO<sub>3</sub> solution at 37 °C for 24 h and then neutralized with 1 N HCl solution to pH 7. The resulting solutions were then subjected to further PL characterization. Quantum yields were determined on the same spectrofluorometer by using a Quantum-φ integrating sphere (Horiba Scientific, Edison NJ) at the same concentration and slit size used with blank solvent as the reference. The photostabilities of small molecules and polymers were determined by monitoring the emission intensity decay at their spectral maximum excitation and emission wavelengths over 3 h of continuous illumination at 1 nm excitation and 1 nm emission bandpass in the spectrofluorometer.

### 2.3. Time-resolved fluorescence spectroscopy

Fluorescence lifetimes were determined by using the Time-Correlation Single Photon Counting (TCSPC) accessory to the FluoroMax-4 (Horiba, NJ). NanoLED pulse light sources at wavelengths of 352 nm and 390 nm were used for excitation. All experiments and data fitting were performed by following manufacturer's manual. For each decay curve, 10,000 photons were collected. Fluorescence lifetime decays were fitted with an exponential series according to Eq. (1) below:

$$F(t) = A + B_1 \exp\left(-\frac{t}{\tau_1}\right) + B_2 \exp\left(-\frac{t}{\tau_2}\right) + B_3 \exp\left(-\frac{t}{\tau_3}\right) + \dots \quad (1)$$

Here,  $F(t)$  is the lifetime decay function with respect to time  $t$ ,  $\tau_i$  is the lifetime value of the emitting species,  $A$  is the background offset, and  $B_i$  is the pre-exponential function of the emitting species. The method of least squares was used to quantify a  $\chi^2$  value based on the decay data and fitting function, where  $\chi^2$  values smaller than 1.2 indicate a good fit, and values above 1.2 indicate a need for multiple exponential fittings according to Eq. (1). If the lifetime decay is dominated by a single emitting species, the equation can be simplified to include only the first two terms. Single exponential fitting was accurate for TPA based fluorophores. However, for DPR based fluorophores, only three exponential fitting gave a  $\chi^2$  value smaller than 1.2 and randomized the residue distribution. In addition,  $B_i$  measures the relative percentage of the specified species with the corresponding lifetime  $\tau_i$ .

### 2.4. Computational modeling

All calculations reported in this work were performed by means of the Gaussian 09 program package [8]. Geometries of all compounds are allowed to fully relax during the B3LYP/6-311++G\*\* optimization process [9]. NICS values were also computed with the B3LYP/6-311++G\*\* method through the gauge-including atomic orbital method (GIAO) implemented in Gaussian 09 [10]. NICS values at the geometrical center of the perpendicular plane of the ring were calculated [11].

To calculate the theoretical absorbance wavelengths, the ground state geometry was optimized with density functional theory B3LYP, at the 6-311G+(d,p) level of theory with a IEFPCM water solvent model, and theoretical absorption spectra were calculated with ZINDO energy calculations by using Gaussian 09 [8].

### 2.5. Protein labeling and cell imaging

To conjugate CA-Cys onto proteins, 1 mg CA-Cys were first dissolved in 10 mL PBS buffer (pH 7.5). Next, 10 mg 1-ethyl-3-(3-dimethylaminopropyl) carbodiimide (EDC) and 10 mg N-hydroxysuccinimide (NHS) were added sequentially to activate the carboxyl groups CA-Cys under stirring for one hour each at room temperature. 40 mg bovine serum albumin (BSA) were dis-

solved in 20 mL PBS solution separately and then added into the activated CA-Cys solution. The mixtures were stirred for four hours at room temperature. The resulting BSA-CA-Cys was purified by dialysis in a bag with molecular weight cut-off (MWCO) of 1000 Dalton against DI water for 24 h at 4 °C and followed by lyophilization. Pristine BSA and CA-Cys labeled BSA were then dissolved in PBS in a concentration of 50 µg/mL and subjected for fluorescence spectrophotometer by using excitation of 365 nm.

For cell imaging, CA-Ala was activated by EDC/NHS in a similar fashion. Briefly, 1 mg CA-Ala was dissolved in 10 ml PBS, and then 10 mg EDC and 10 mg NHS were added sequentially and reacted for 1 h each at room temperature. Next, the mixture was purified by dialysis against DI water in a dialysis bag of 500 MWCO for 24 h and lyophilized. For cell culture, NIH 3T3 mouse fibroblast was selected as a model. 3T3 cells were cultured in Dulbecco's Modified Eagle's Medium (DMEM) supplemented with 10% FBS and 1% penicillin-streptomycin (1–100 dilution of 100× stock solution in DMEM) at 37 °C under 5% CO<sub>2</sub>. Then, 10<sup>4</sup> cells were seeded onto a cover slip and washed by PBS after 24 h. NHS-CA-Ala was added with a final concentration of 100 µg/mL and allowed to bind to cells for 2 h. Afterwards, 3T3 fibroblasts were washed gently by PBS for three times and fixed by 4% paraformaldehyde for 30 min. 4',6-Diamidino-2-Phenylindole (DAPI) was used to stain the nuclei of 3T3 cells. Finally, the cells were imaged by using an Olympus Fluorview 100 confocal microscope and the excitation/emission settings for fluorescein isothiocyanate (FITC).

### 3. Results and discussion

In this work, synthesis routes and chemical structures of CPDs are summarized in Scheme 1. Unlike many traditional organic dyes, most CPDs are water soluble as made, due to the presence of carboxyl groups from citric acid. As shown in Scheme 1, the first type of CPD was synthesized from citric acid and β-/γ-aminothiols and the second type was generated from citric acid and primary amines without a thiol group. The former type is represented by dye synthesized from citric acid and L-cysteine, referred to as CA-Cys; the latter is represented by dye synthesized from citric acid and L-alanine, referred to as CA-Ala. Our facile synthesis strategies produce yields of 34% for CA-Cys and 28.9% for CA-Ala. The structures and photophysical properties of the synthesized CPDs are summarized in Table S1.

#### 3.1. Synthesis and fluorescent properties of thiazolo pyridine carboxylic acid based dyes

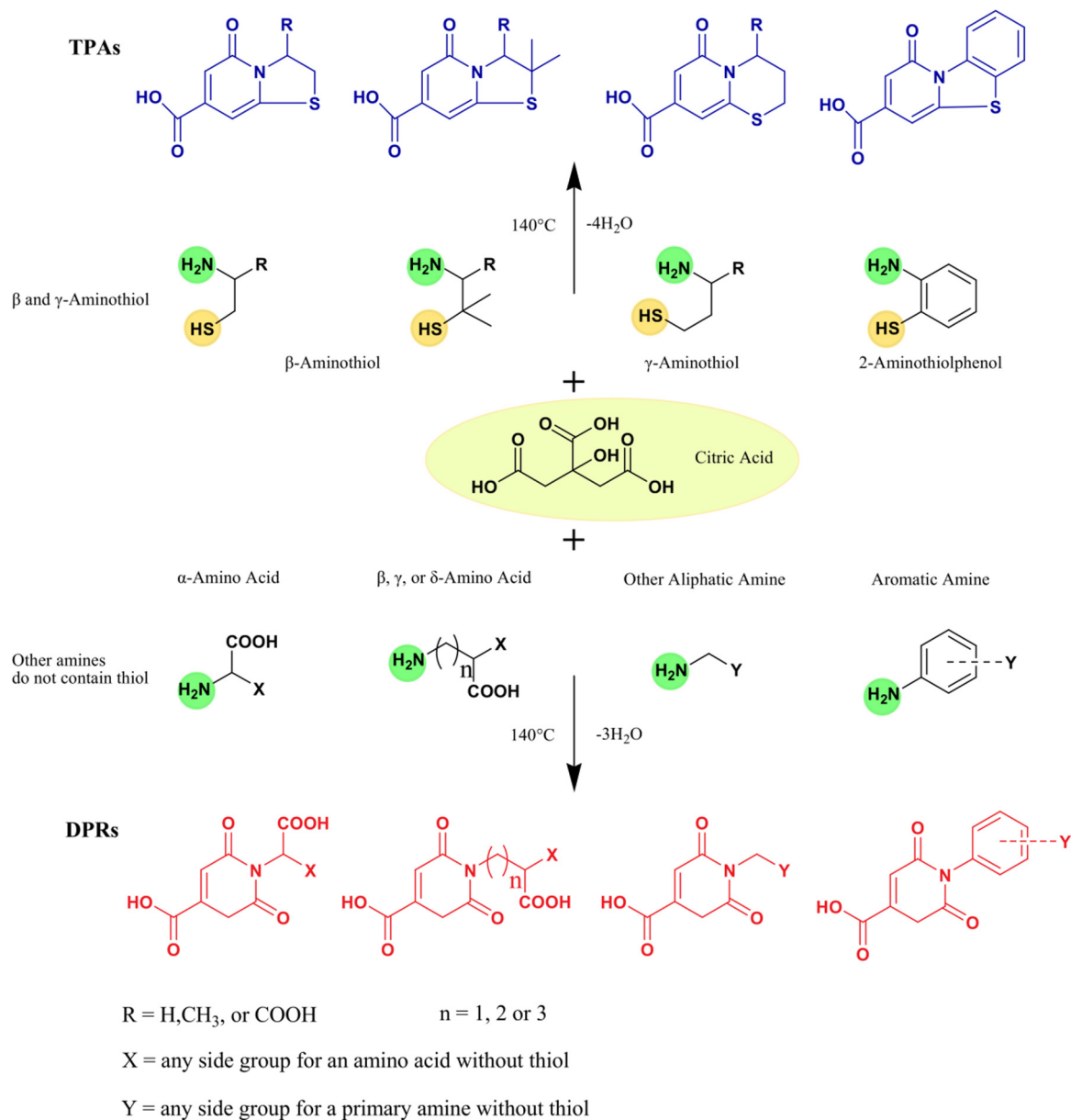
To synthesize the first class of CPDs, equimolar amounts of citric acid and β-/γ-aminothiols were reacted, resulting in a thiazolo pyridine carboxylic acid (TPA) (Figs. 1a and S4). TPA structures were first reported by Kasprzyk and co-workers, however, the fluorescence mechanism have not been studied in details [12]. As an example, CA-Cys showed strong fluorescence with quantum yields as high as 81% and an extinction coefficient of 8640 M<sup>-1</sup> cm<sup>-1</sup>, resulting in strong fluorescence that can even be observed under white light (Fig. 1c). The emission peak of CA-Cys remained fixed at 430 nm independent of the wavelength of excitation. In other words, band-shifting behavior, defined as fluorescence emission peak shifting with different excitation wavelengths (Fig. 1b), was not observed [7]. This behavior is marked by the approximate symmetry of the 3D fluorescence spectra. In these cases, fluorescence results from the relaxation of the electronically excited singlet state in its lowest vibrational energy level to the ground state (Kasha's Rule) [13]. By reacting citric acid with other β- or γ-aminothiols including homocysteine, cysteamine, and penicil-

lamine, similarly strong fluorescence emissions lacking band shifting behavior were observed (Figs. S1–S3). In addition, simply by adding an aliphatic diol into the reaction, we can produce biodegradable photoluminescent polymers (BPLP), reported previously [7]. For instance, BPLP-Cys showed fluorescence properties similar to CA-Cys and *in vivo* degradability [14].

Since the fluorescence of most organic dyes stems from conjugated aromatic rings [4,15], we next calculated the aromaticity of TPA molecules based on the Nucleus Independent Chemical Shift (NICS) model [16,17]. The class of TPAs including CA-Cys, CA-Cysteamine, and CA-Homocysteine all demonstrated high aromaticity with NICS < -3.0 (Table S2). Thus, the fluorescence mechanism of TPAs resembles that of most organic dyes, whose fluorescence results from π-π\* electronic excitation that leads to emission from the lowest energy band. The time-dependent fluorescence of CA-Cys can be fitted to a single-exponential decay, resulting in a single lifetime of τ = 9.86 ± 0.078 ns (Fig. S38). Thus the fluorescence emission of TPA molecules obeys Kasha's rule, as illustrated by a Jablonski diagram (Fig. S5).

#### 3.2. Synthesis and fluorescent properties of dioxo-pyridine ring based dyes

The second type of CPDs was made from citric acid and amines lacking a thiol group by the same simple solvent-free reaction (Scheme 1). A dioxo-pyridine ring (DPR) structure was identified as the fluorophore, exemplified by CA-Ala (Figs. 2a and S8). Some DPRs, for example CA-Gly, showed minor impurities in NMR, suggesting that the purification may need to be further improved. Compared to TPAs, DPRs exhibited relatively weak fluorescence with quantum yields lower than 40%, as well as distinct band shifting of emission and varying Stokes Shifts that were dependent on the excitation wavelengths (Figs. 2b, S9 and S10). Moreover, unlike TPAs, DPRs do not have conjugated structures, as supported by low aromaticity with NICS > 1.5 (Table S2). Thus, the fluorescence mechanism of conventional conjugated organic dyes is not applicable here, and DPR likely represents a distinct PL mechanism [18]. We hypothesized that the aliphatic tertiary nitrogen is the source of fluorescence, as previously suggested for PAMAM dendrimers [19,20]. In an early study, monovalent tertiary amines in gas phase showed emissions limited to the range of 250–400 nm [21,22]. Interestingly, DPRs, PAMAM dendrimers [19,20,23], and amine-containing carbon dots [6,24] all exhibit maximum excitation at 350–380 nm, and maximum emission at 420–450 nm with significantly stronger intensity in the liquid phase. This dichotomy poses an interesting question of how the mechanism of red shift and increased fluorescence of DPRs in the liquid phase differs from that of monovalent tertiary amines in the gas phase [21,22,25]. We propose that both phenomena can be explained by the same mechanism: n-π\* and n-σ\* transitions of the lone pair electrons of the tertiary amine undergo a red-shift due to the electron withdrawing effects of the adjacent carbonyl groups, resulting in stronger visible fluorescence. Indeed, both electron-withdrawing carbonyl groups extend resonance from the tertiary amine, as depicted in the computed isosurfaces in Table 1, resulting in a red shift of absorbance from a smaller highest occupied and lowest unoccupied molecular orbital (HOMO-LUMO) gap. Calculations showed an absorption peak of 263 nm for the tetrahydropyridine lacking both carbonyl groups (molecule 4), which shifted to 303 nm/325 nm (2 and 3), and then to 333 nm (1) with each addition of a carbonyl group. These results provide insight into the fluorescence red shifting behavior of DPRs, and the same mechanism can be used to explain the behavior of PAMAM dendrimers [26] that similarly have carbonyl groups pulling electrons from tertiary amines.



**Scheme 1.** The synthetic routes and structures of CPDs. TPAs (blue) are synthesized by reacting citric acid with  $\beta$  or  $\gamma$ -aminothiols such as cysteine, cysteamine, 2-aminothiophenol, etc. DPRs (red) are synthesized from citric acid and other primary amines/anilines that do not contain a thiol group, e.g. alanine,  $\gamma$ -Aminobutyric acid, propylamine, ethylenediamine, ethanolamine, phenylenediamine, and others. All chiral molecules used were *L*-isomers unless specifically stated otherwise. (For interpretation of the references to colour in this figure legend, the reader is referred to the web version of this article.)

### 3.3. Band shifting of DPRs

More interestingly, all DPRs showed dynamic Stokes shifts and excitation-dependent emission wavelengths, referred to as “band shifting behavior”. For instance, the 3D fluorescence spectra of CA-Ala (Fig. 2b) is not symmetrical as expected for typical fluorophores, but marked by a clear “tail” that expands to longer wavelengths. Similar band shifting behavior, which breaks Kasha’s Rule, has also been found in PAMAM dendrimers [27], carbon dots [6], and graphene oxide [28]. To unveil the mechanism of the band shifting phenomenon of DPRs, time-resolved fluorescence spectroscopy was performed. First, the fluorescence decay of CA-Ala cannot be fitted to either a single- or double-exponential decay as the residue distribution is not random (Figs. S39 and S40), suggesting the presence of multiple excited state energy levels that give fluorescence. A triple exponential model adequately (meaning  $\chi^2 < 1.2$  and the residue distributions are random) fits the lifetime

decay (Fig. S41), resulting in  $\tau_1 = 1.03 \pm 0.029$  ns,  $\tau_2 = 4.33 \pm 0.128$  ns, and  $\tau_3 = 10.07 \pm 0.031$  ns. Multiple lifetimes indicate that the fluorescence emission of CA-Ala is not from a single energy band. Thus, we hypothesize that the band shifting phenomenon is a result of the “red edge effect”, where the presence of rotating auxochromic groups generates additional dipole interactions between the fluorophore and solvent during intersystem relaxation, prolonging the solvation time to the approximate time-scale of fluorescence emission [29,30]. As illustrated in Fig. S12, longer solvation time further relaxes the excited state to various lower energy levels, resulting in multiple lifetimes and red-shifting emissions. The absence of band shifting seen in TPA can be explained by its non-rotating highly conjugated auxochromic ring structure. In the cases of TPA and other conjugated organic dyes, the solvation times,  $\tau_s$ , are normally around 10 ps, which are considerably shorter than the fluorescence lifetimes ( $\tau$ ), which are in the range of 0.5–30 ns [31]. In contrast, non-aromatic DPR

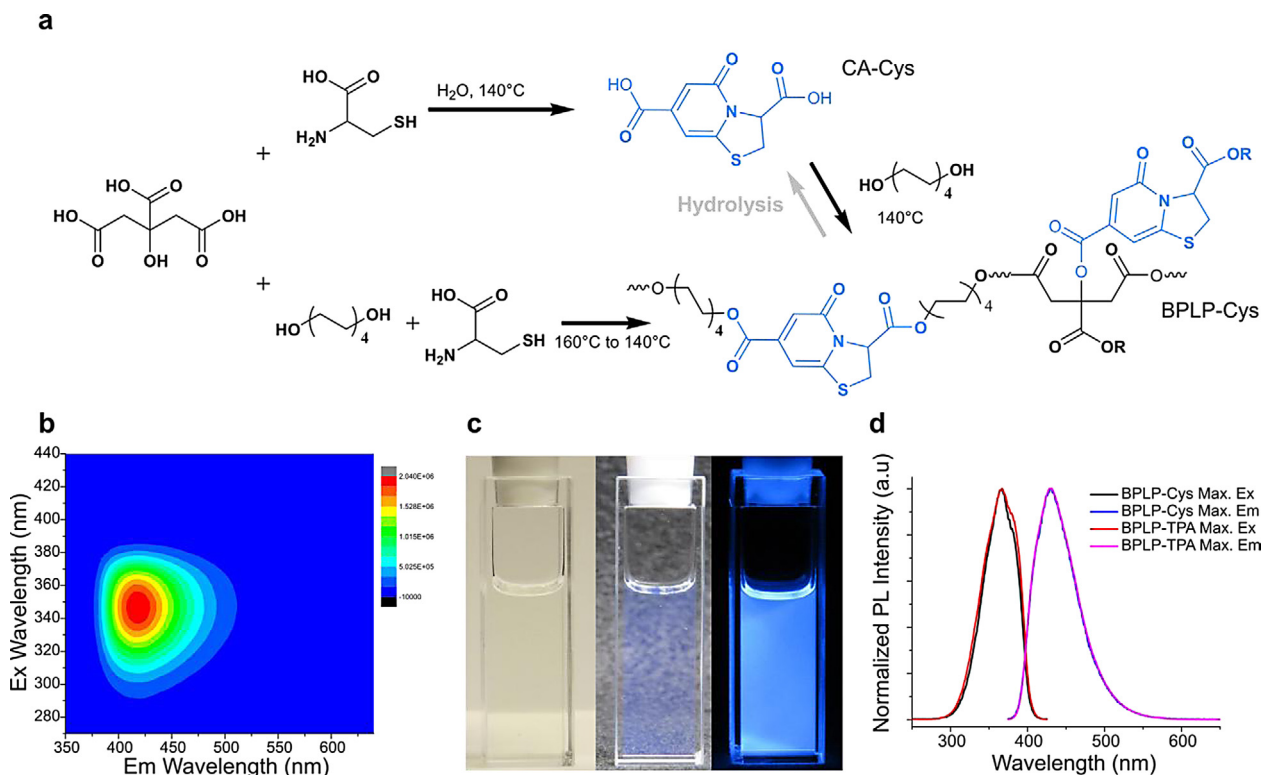


**Fig. 1.** Synthesis and fluorescence properties of CA-Cys and BPLP-Cys. (a) Synthetic schemes for CA-Cys (from citric acid and cysteine), BPLP-Cys (from citric acid, 1,8-octanediol, and cysteine), and BPLP-TPA (from CA-Cys and 1,8-octanediol). The hydrolysis reaction of BPLP-Cys to form CA-Cys is also illustrated. (b) 3D excitation-emission spectra of CA-Cys in water solution. (c) Images of CA-Cys solution under white light with white/black background and under UV light (from left to right). (d) Comparison of maximum excitation and emission spectra of BPLP-Cys and BPLP-TPA (which resulted from the reaction of CA-Cys and 1,8-octanediol).

possesses rotating auxochromic groups, and thus solvation may be allowed to  $\tau_s \approx \tau$  in polar solvents. Furthermore, the solvation process of DPR explains our earlier observations, such as the relatively low quantum yields of DPRs (Table S1), as well as the presence of at least three distinct lifetimes for CA-Ala compared to a single lifetime for CA-Cys.

To prove that the dynamic band shifting exhibited by DPRs is indeed generated by the red-edge effect, we demonstrate a correlation between the band shifting and solvent polarity. The relaxation kinetics of DPRs were measured by the extent of band shift (Fig. 3a–c) and fluorescence lifetimes (Fig. 3d–f). The extent of band shift (i.e. intensity of emission at longer wavelengths) is shown to increase with solvent polarity, as the band-shift effect of CA-Ala is strongest in water (dielectric constant  $\epsilon = 80.1$ ), moderate in acetone ( $\epsilon = 20.7$ ), and minimal in non-polar solvents such as dichloromethane ( $\epsilon = 8.93$ ) (Fig. 3a–c). Interestingly, when fluorescence lifetime decays of CA-Ala were collected at different emission wavelengths, the decay plots varied significantly in water (Fig. 3d), changed slightly in acetone (Fig. 3e), but remained relatively constant in dichloromethane (Fig. 3f). As the fluorescence emission wavelengths represent the band edge energy levels that correspond to the allowed timescale of solvent relaxation, the lifetimes of CA-Ala in polar solvents responded dynamically to the extent of solvent relaxation [28,32]. As a result, the relaxation kinetics of DPRs is largely influenced by dipole alignments in response to polar solvents [28,29]. The effect of solvent also can be observed in the 3D spectra of polymeric BPLP-Ala (Fig. 2c), which is dissolved in 1,4-dioxane. Furthermore, the band shifting of BPLP-Ala is clearly not as strong as CA-Ala in water solution (Fig. 2b). Thus, the band shifting of DPR is caused by the red-edge effect, which is ultimately governed by fluorophore/solvent interactions.

### 3.4. Photostability of citric acid-derived photoluminescent dyes

In addition to the photoluminescent behavior discussed above, CPDs have the advantages of high photostability and long lifetimes. Just as high photostability was previously reported in BPLPs [14,33], CA-Cys was found to be extremely stable, with 95% of the fluorescence intensity remaining after continuous UV excitation for 3 h (Fig. 4a). In contrast, DPRs such as CA-Ala showed photobleaching on par with Fluorescein, but were more resistant to photobleaching than Rhodamine B. We propose that the high photostability of TPA structures arises from the presence of efficient deactivation pathways of photoexcited molecules along the 2-pyridone fused ring structure, much like the deactivation pathways studied in adenine [34,35]. Such internal conversion pathways through out-of-plane modes of vibrations are reportedly efficient and lead to high photostability [35], whereas inefficient radiationless deactivation of excited DPR molecules may arise from solvent relaxation processes due to rotation of the auxiliary group, resulting in lower photostability. When excited by a pulsed laser, CPDs, including both CA-Cys and CA-Ala, exhibited longer emission decay lifetimes than Rhodamine B and Fluorescein (Fig. 4b). Long lifetimes are typically found in blue dyes; however, the band shifting exhibited by DPRs (exemplified by CA-Ala) may have potential for use in fluorescence lifetime imaging (FLIM) of biological tissues and molecules [36].

### 3.5. Applications of CPDs

Fluorescent dyes have wide applications ranging from molecular labeling to *in vivo* imaging. To demonstrate the potential applications of our newly-developed CPDs, we first conjugated bovine serum albumin (BSA), as a representative biomolecule, with CA-

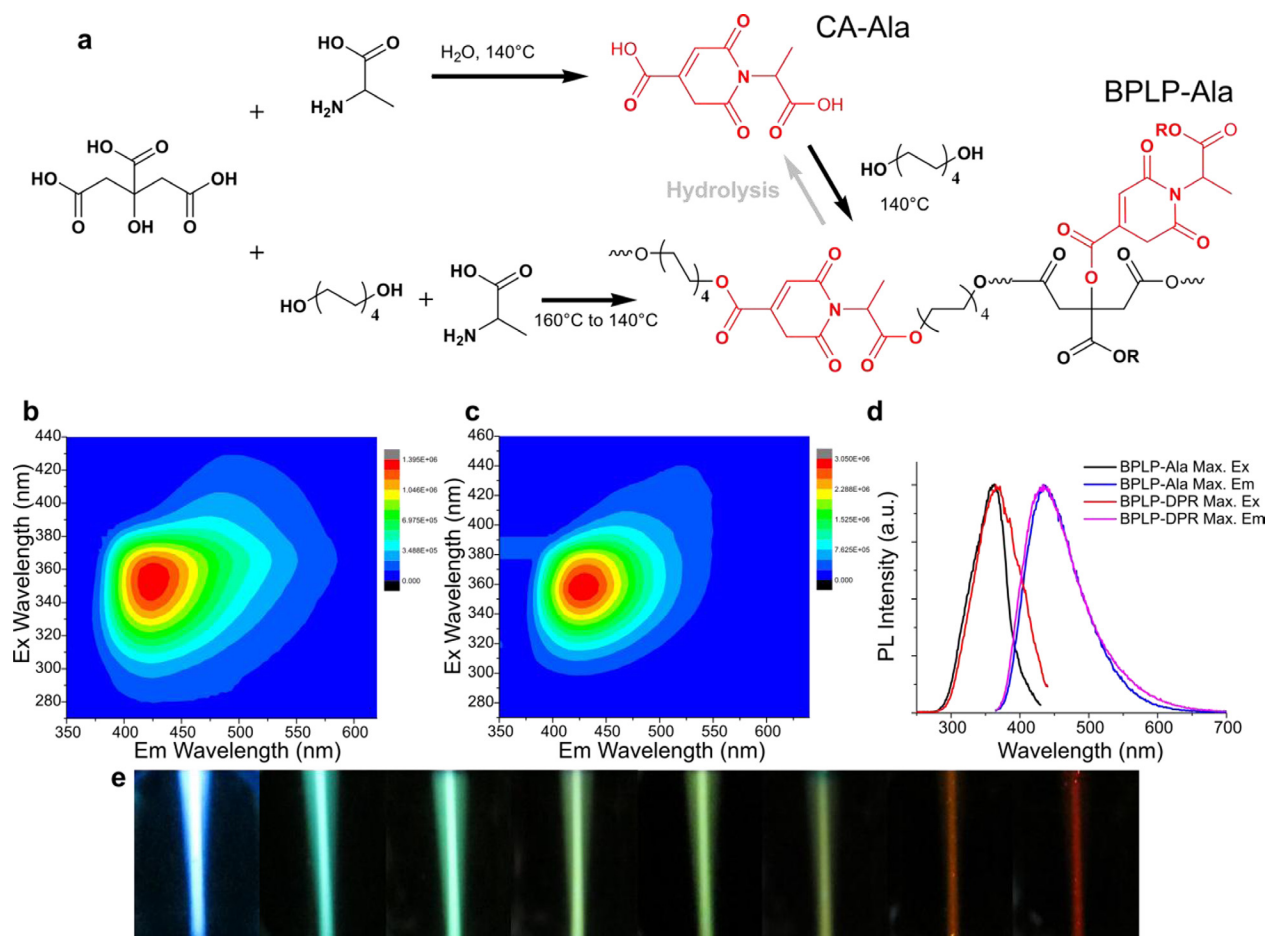


**Fig. 2.** Synthesis and fluorescence properties of CA-Ala and BPLP-Ala. (a) Synthesis schemes of CA-Ala (from citric acid and alanine), BPLP-Ala (from citric acid, 1,8-octanediol, and Alanine), and BPLP-DPR (from CA-Ala and 1,8-octanediol). The hydrolysis reaction of BPLP-Ala resulting in CA-Ala is also illustrated. (b) 3D excitation-emission spectra of CA-Ala in water solution. (c) 3D excitation-emission spectra of BPLP-Ala in 1,4-dioxane solution. (d) Comparison of excitation and emission spectra of BPLP-Ala and BPLP-DPR-Ala. (e) Optical images of BPLP-Ala solutions at increasing excitation wavelengths from left to right.

Cys. The free carboxyl groups of our CPDs enable facile conjugation by carbodiimide chemistry to produce a wide range of molecular labels. As shown in Fig. 5a, strong blue fluorescence can be observed from purified CA-Cys conjugated BSA molecules. We were able to establish a calibration curve of CA-Cys labeled BSA to quantify the BSA concentration as well (data not shown). In addition, the carboxyl groups on CPDs are also available for modification in cellular labeling. For example, CA-Ala with activated carboxyl groups were used to label fibroblasts, and imaged using confocal microscopy (Fig. 5b). Fibroblasts labeled by CA-Ala showed strong green fluorescence in the FITC channel, owed to the band shifting behavior of CA-Ala. It is clear that CPDs have potential in cellular imaging, tracing and visualization.

### 3.6. CPD and biodegradable photoluminescent polymer

The discovery of CPDs not only establishes a new family of fluorophores, but it also provides insight into the fluorescence mechanism of our previously developed biodegradable photoluminescent polymers (BPLPs) that were synthesized by directly reacting citric acid, an amino acid such as L-cysteine, and a diol such as 1,8-octanediol [7]. Previously, our group has demonstrated the applications of BPLPs in tissue engineering, bioimaging, theranostic drug delivery, and more recently, selective halide (chloride, bromide, iodide) sensing for fluorescence based diagno-

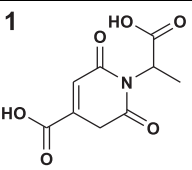
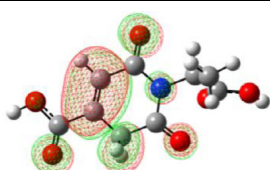
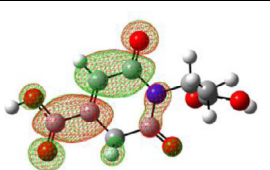
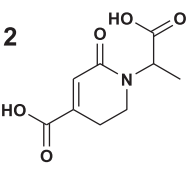
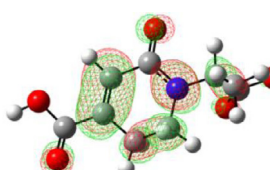
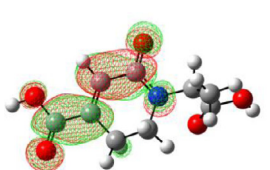
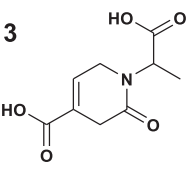
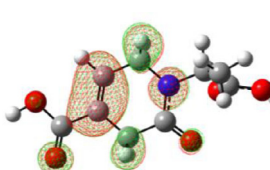
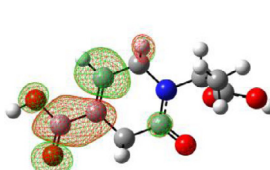
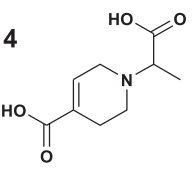
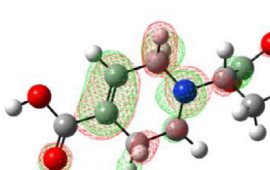
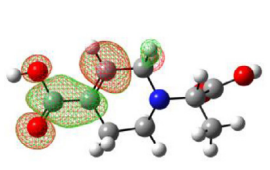
sis of cystic fibrosis [7,14,37,38]. To establish that the TPA structure is indeed the fluorescent moiety of BPLPs, we synthesized polymers by reacting purified CA-Cys with 1,8-octanediol. The PL properties of the resultant BPLP-TPA were identical to that of BPLP-Cys synthesized by reacting citric acid, 1,8-octanediol, and L-cysteine directly (Fig. 1d), including a lack of band-shifting (Fig. S6). Additionally, CA-Ala could be directly reacted with 1,8-octanediol to form a BPLP-DPR whose PL properties were very similar to that of CA-Ala (Fig. 2d). Moreover, CA-Cys and CA-Ala were found in the alkaline hydrolysis products of BPLP-Cys and BPLP-Ala, respectively, which confirmed that the fluorophores of BPLPs are indeed CPDs. (Figs. S7 and S11).

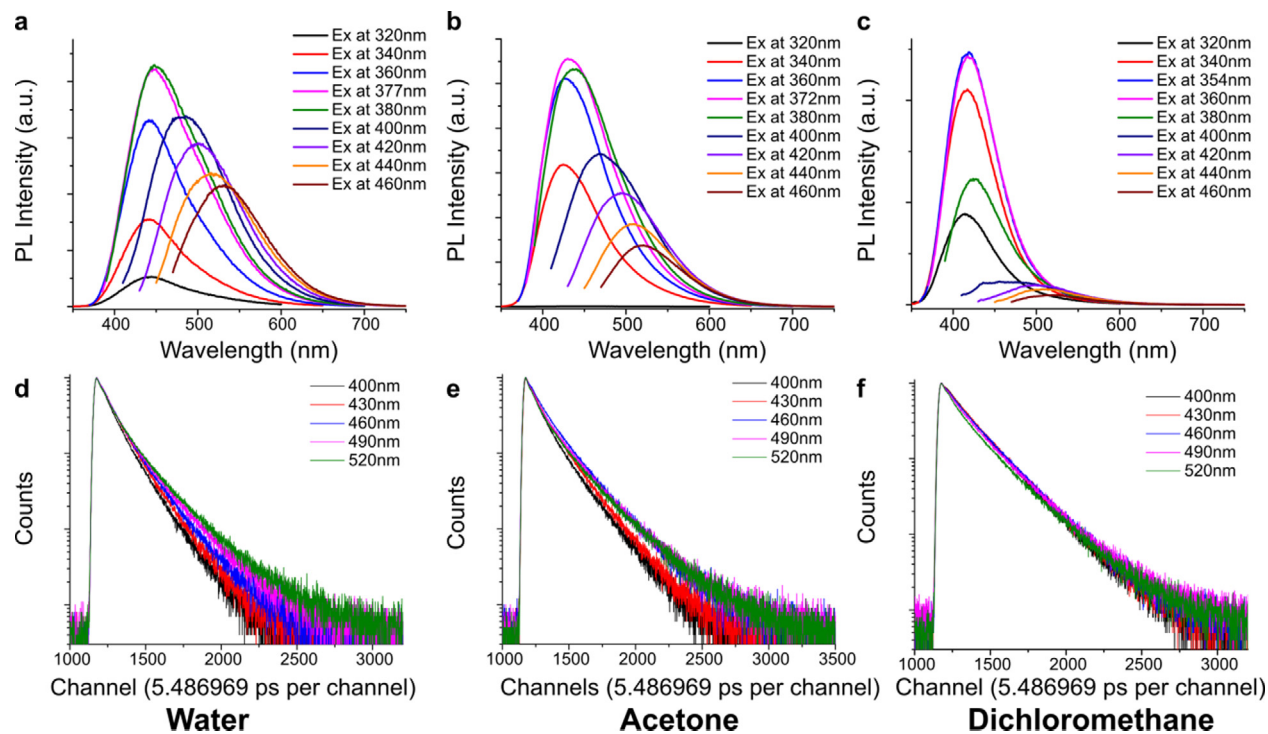
## 4. Conclusions

In summary, we have synthesized a series of citric acid-derived fluorophores and determined their mechanisms of fluorescence. The primary approach for generating citric acid derived photoluminescent dyes (CPDs) is by reacting citric acid with primary amine-containing molecules. If the primary amines used in the reaction are  $\beta$  or  $\gamma$ -aminothiol, conjugated TPA structures will be synthesized, exhibiting strong fluorescence emission with high quantum yield, single-exponential lifetimes, and absence of band shifting behavior. If primary amines without thiol groups are used to react with citric acid, non-conjugated DPRs will be synthesized, emitting

**Table 1**

Computed absorption peak wavelengths and isosurfaces of LUMO for CA-Ala and its analogs without one or two carbonyl groups.

Structure	Absorption wavelength	Isosurfaces of HOMO	Isosurfaces of LUMO
<b>1</b> 	333 nm		
<b>2</b> 	303 nm		
<b>3</b> 	325 nm		
<b>4</b> 	263 nm		

**Fig. 3.** (a–c) Fluorescence emission spectra of CA-Ala at different excitation wavelengths in water, acetone and dichloromethane. (d–f) Fluorescence intensity–time traces of CA-Ala at different emission wavelengths in water, acetone and dichloromethane.

fluorescence with relatively lower quantum yields, multiple lifetimes, band shifting behavior, and dynamic Stokes shifts. We also demonstrate that CPDs can be used as fluorescent molecules to

react with other monomers to form fluorescent polymers supported by the syntheses of BPLP-TPAs and BPLP-DPRs. In conclusion, we have established a methodology to design and prepare

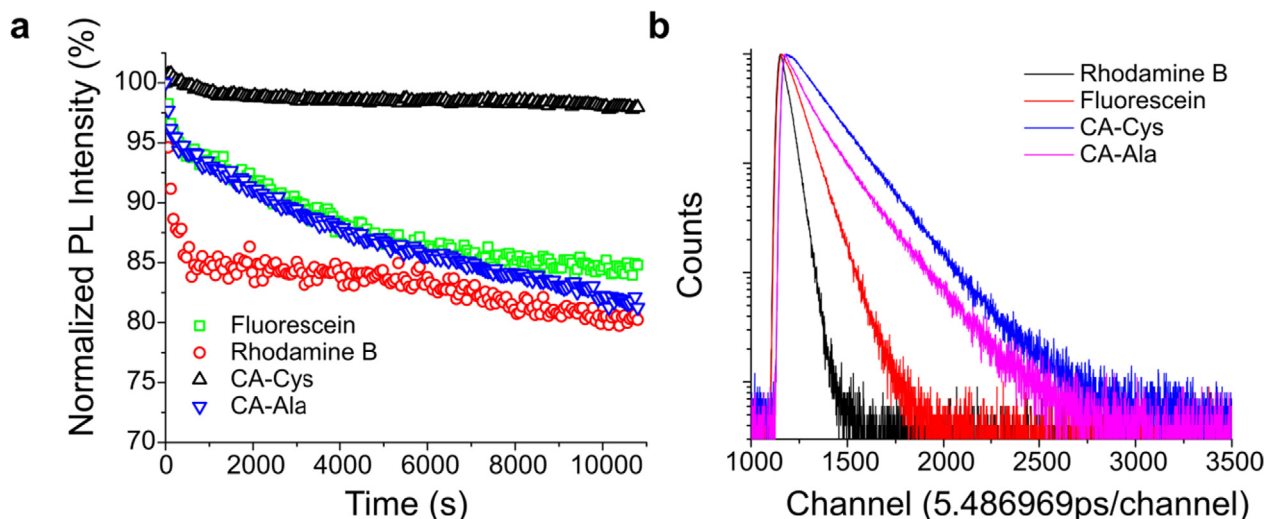


**Fig. 4.** (a) Fluorescence photostabilities of CA-Cys and CA-Ala with 3 h continuous excitation at their respective maximums. Fluorescein and Rhodamine B served as controls. (b) Fluorescence intensity–time traces of CA-Cys, CA-Ala, Fluorescein and Rhodamine B after pulsed excitation at 352 nm.

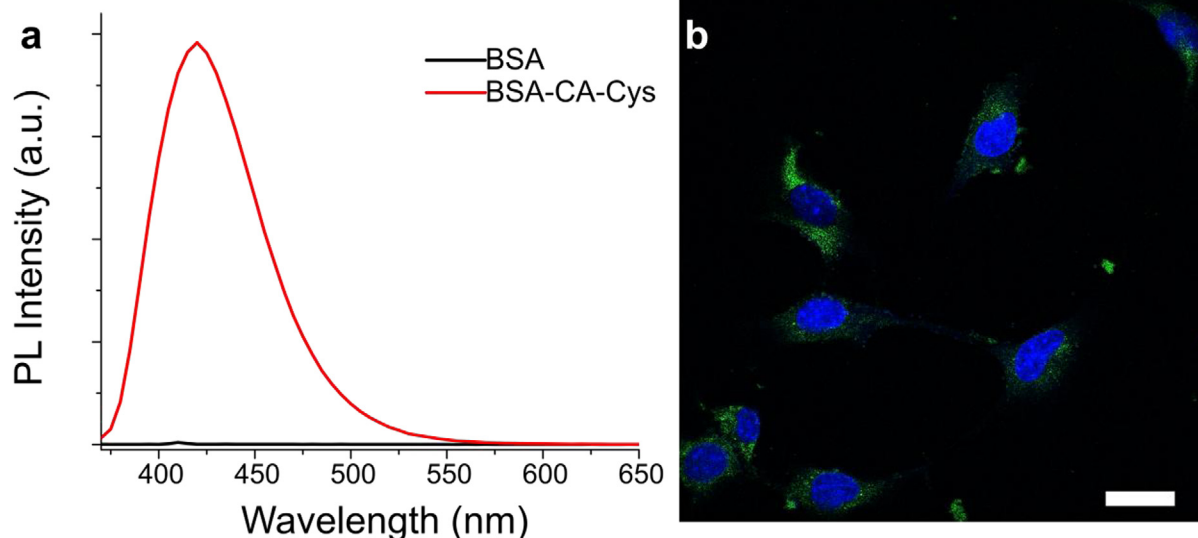


**Fig. 5.** (a) Emission spectra of BSA and CA-Cys labeled BSA solutions in PBS, excited at 365 nm. (b) Confocal microscope image of 3T3 fibroblasts, stained by NHS activate CA-Ala (imaged under FITC filter) and DAPI. Scale bar = 30  $\mu$ m.

new fluorescent dyes and polymers derived from citric acid and amine-containing molecules in an extremely facile and low-cost manner, to meet the ever-growing needs in applications where fluorescence is an enabling tool.

## Notes

Dr. Yang and The Pennsylvania State University have a financial interest in Aleo BME, Inc. These interests have been reviewed by the University's Institutional and Individual Conflict of Interest Committees and are currently being managed by the University.

## Acknowledgements

The authors acknowledge the financial support from National Institutes of Health (NIH – United States) Awards (NIBIB EB012575, NCI CA182670, NHLBI HL118498), and National Science Foundation (NSF – United States) Awards (DMR1313553).

## Appendix A. Supplementary data

Supplementary data associated with this article can be found, in the online version, at <http://dx.doi.org/10.1016/j.actbio.2017.01.019>.

## References

- [1] M. Fernandez-Suarez, A.Y. Ting, Fluorescent probes for super-resolution imaging in living cells, *Nat. Rev. Mol. Cell Biol.* 9 (12) (2008) 929–943.
- [2] F. Wang, W.B. Tan, Y. Zhang, X.P. Fan, M.Q. Wang, Luminescent nanomaterials for biological labelling, *Nanotechnology* 17 (1) (2006) R1–R13.
- [3] M.Y. Berezin, S. Achilefu, Fluorescence lifetime measurements and biological imaging, *Chem. Rev.* 110 (5) (2010) 2641–2684.
- [4] U. Resch-Genger, M. Grabolle, S. Cavaliere-Jaricot, R. Nitschke, T. Nann, Quantum dots versus organic dyes as fluorescent labels, *Nat. Methods* 5 (9) (2008) 763–775.
- [5] P. Ferruti, M.A. Marchisio, R. Duncan, Poly(amido-amine)s: biomedical applications, *Macromol. Rapid Commun.* 23 (5–6) (2002) 332–355.
- [6] S. Zhu, Q. Meng, L. Wang, J. Zhang, Y. Song, H. Jin, K. Zhang, H. Sun, H. Wang, B. Yang, Highly photoluminescent carbon dots for multicolor patterning, sensors, and bioimaging, *Angew. Chem. Int. Ed.* 52 (14) (2013) 3953–3957.

- [7] J. Yang, Y. Zhang, S. Gautam, L. Liu, J. Dey, W. Chen, R.P. Mason, C.A. Serrano, K. A. Schug, L. Tang, Development of aliphatic biodegradable photoluminescent polymers, *Proc. Natl. Acad. Sci. U.S.A.* 106 (25) (2009) 10086–10091.
- [8] M.J. Frisch, G.W. Trucks, H.B. Schlegel, G.E. Scuseria, M.A. Robb, J.R. Cheeseman, G. Scalmani, V. Barone, B. Mennucci, G.A. Petersson, H. Nakatsuji, M. Caricato, X. Li, H.P. Hratchian, A.F. Izmaylov, J. Bloino, G. Zheng, J.L. Sonnenberg, M. Hada, M. Ehara, K. Toyota, R. Fukuda, J. Hasegawa, M. Ishida, T. Nakajima, Y. Honda, O. Kitao, H. Nakai, T. Vreven, J.A. Montgomery Jr., J.E. Peralta, F. Ogliaro, M.J. Bearpark, J. Heyd, E.N. Brothers, K.N. Kudin, V.N. Staroverov, R. Kobayashi, J. Normand, K. Raghavachari, A.P. Rendell, J.C. Burant, S.S. Iyengar, J. Tomasi, M. Cossi, N. Rega, N.J. Millam, M. Klene, J.E. Knox, J.B. Cross, V. Bakken, C. Adamo, J. Jaramillo, R. Gomperts, R.E. Stratmann, O. Yazyev, A.J. Austin, R. Cammi, C. Pomelli, J.W. Ochterski, R.L. Martin, K. Morokuma, V.G. Zakrzewski, G.A. Voth, P. Salvador, J.J. Dannenberg, S. Dapprich, A.D. Daniels, Ö. Farkas, J.B. Foresman, J.V. Ortiz, J. Cioslowski, D.J. Fox, Gaussian 09, Gaussian Inc: Wallingford, CT, USA, 2009.
- [9] R. Krishnan, J.S. Binkley, R. Seeger, J.A. Pople, Self-consistent molecular orbital methods. XX. A basis set for correlated wave functions, *J. Chem. Phys.* 72 (1) (1980) 650–654.
- [10] R. Ditchfield, W.J. Hehre, J.A. Pople, Self-consistent molecular-orbital methods. IX. An extended Gaussian-type basis for molecular-orbital studies of organic molecules, *J. Chem. Phys.* 54 (2) (1971) 724–728.
- [11] J. Kruszewski, T.M. Krygowski, Definition of aromaticity basing on the harmonic oscillator model, *Tetrahedron Lett.* 13 (36) (1972) 3839–3842.
- [12] W. Kasprzyk, S. Bednarz, D. Bogdał, Luminescence phenomena of biodegradable photoluminescent poly (diol citrates), *Chem. Commun.* 49 (57) (2013) 6445–6447.
- [13] A.N. Fletcher, Fluorescence emission band shift with wavelength of excitation, *J. Phys. Chem.* 72 (8) (1968) 2742–2749.
- [14] Z. Xie, Y. Zhang, L. Liu, H. Weng, R.P. Mason, L. Tang, K.T. Nguyen, J.-T. Hsieh, J. Yang, Development of intrinsically photoluminescent and photostable polylactones, *Adv. Mater.* 26 (26) (2014) 4491–4496.
- [15] G. Ulrich, R. Ziessel, A. Harriman, The chemistry of fluorescent bodipy dyes: versatility unsurpassed, *Angew. Chem. Int. Ed.* 47 (7) (2008) 1184–1201.
- [16] P.V.R. Schleyer, C. Maerker, A. Dransfeld, H. Jiao, N.J.R.v.E. Hommes, Nucleus-independent chemical shifts: a simple and efficient aromaticity probe, *J. Am. Chem. Soc.* 118 (26) (1996) 6317–6318.
- [17] A. Stanger, Nucleus-independent chemical shifts (NICS): distance dependence and revised criteria for aromaticity and antiaromaticity, *J. Org. Chem.* 71 (3) (2005) 883–893.
- [18] R.L. Joseph, *Principle of Fluorescence Microscopy*, Springer Science + Business Media, LLC, New York, NY, 2006.
- [19] D. Wang, T. Imae, Fluorescence emission from dendrimers and its pH dependence, *J. Am. Chem. Soc.* 126 (41) (2004) 13204–13205.
- [20] M. Sun, C.-Y. Hong, C.-Y. Pan, A unique aliphatic tertiary amine chromophore: fluorescence, polymer structure, and application in cell imaging, *J. Am. Chem. Soc.* 134 (51) (2012) 20581–20584.
- [21] A.M. Halpern, T. Gartman, Structural effects on photophysical processes in saturated amines. II, *J. Am. Chem. Soc.* 96 (5) (1974) 1393–1398.
- [22] R.A. Beecroft, R.S. Davidson, T.D. Whelan, Fluorescent excimer formation by alpha, omega-diaminoalkanes and related compounds, *J. Chem. Soc. Perkin Trans. 2* (7) (1985) 1069–1072.
- [23] G. Jiang, X. Sun, Y. Wang, M. Ding, Synthesis and fluorescence properties of hyperbranched poly(amidoamine)s with high density tertiary nitrogen, *Polym. Chem.* 1 (10) (2010) 1644–1649.
- [24] S. Sahu, B. Behera, T.K. Maiti, S. Mohapatra, Simple one-step synthesis of highly luminescent carbon dots from orange juice: application as excellent bio-imaging agents, *Chem. Commun.* 48 (70) (2012) 8835–8837.
- [25] C.G. Freeman, M.J. McEwan, R.F.C. Claridge, L.F. Phillips, Fluorescence of aliphatic amines, *Chem. Phys. Lett.* 8 (1) (1971) 77–78.
- [26] D. Wang, T. Imae, M. Miki, Fluorescence emission from PAMAM and PPI dendrimers, *J. Colloid Interface Sci.* 306 (2) (2007) 222–227.
- [27] W. Yang, C.-Y. Pan, Synthesis and fluorescent properties of biodegradable hyperbranched poly(amido amine)s, *Macromol. Rapid Commun.* 30 (24) (2009) 2096–2101.
- [28] S.K. Cushing, M. Li, F. Huang, N. Wu, Origin of strong excitation wavelength dependent fluorescence of graphene oxide, *ACS Nano* 8 (1) (2013) 1002–1013.
- [29] A.P. Demchenko, The red-edge effects: 30 years of exploration, *Luminescence* 17 (1) (2002) 19–42.
- [30] A. Samanta, Dynamic Stokes shift and excitation wavelength dependent fluorescence of dipolar molecules in room temperature ionic liquids, *J. Phys. Chem. B* 110 (28) (2006) 13704–13716.
- [31] L. Reynolds, J.A. Gardecki, S.J.V. Frankland, M.L. Horng, M. Maroncelli, Dipole solvation in nondipolar solvents: experimental studies of reorganization energies and solvation dynamics, *J. Phys. Chem.* 100 (24) (1996) 10337–10354.
- [32] S.K. Cushing, M. Li, F. Huang, N. Wu, Origin of strong excitation wavelength dependent fluorescence of graphene oxide, *ACS Nano* 8 (1) (2014) 1002–1013.
- [33] Y. Zhang, J. Yang, Design strategies for fluorescent biodegradable polymeric biomaterials, *J. Mater. Chem. B* 1 (2) (2013) 132–148.
- [34] C. Canuel, M. Mons, F. Piuze, B. Tardivel, I. Dimicoli, M. Elhanine, Excited states dynamics of DNA and RNA bases: characterization of a stepwise deactivation pathway in the gas phase, *J. Chem. Phys.* 122 (7) (2005) 074316.
- [35] Andrzej L. Sobolewski, Wolfgang Domcke, The chemical physics of the photostability of life, *Europhys. News* 37 (4) (2006) 20–23.
- [36] W. Becker, Fluorescence lifetime imaging – techniques and applications, *J. Microsc.* 247 (2) (2012) 119–136.
- [37] J.P. Kim, Z. Xie, M. Creer, Z. Liu, J. Yang, Citrate-based fluorescent materials for low-cost chloride sensing in the diagnosis of cystic fibrosis, *Chem. Sci.* 8 (2017) 550–558.
- [38] Y. Zhang, R.T. Tran, I.S. Qattan, Y.-T. Tsai, L. Tang, C. Liu, J. Yang, Fluorescence imaging enabled urethane-doped citrate-based biodegradable elastomers, *Biomaterials* 34 (16) (2013) 4048–4056.

# SUPPORTING INFORMATION

## Synthesis and characterization of citrate-based fluorescent small molecules and biodegradable polymers

Zhiwei Xie,<sup>a</sup> Jimin P. Kim,<sup>a</sup> Qing Cai,<sup>b</sup> Yi Zhang,<sup>c</sup> Jinshan Guo,<sup>a</sup> Ranjodh S. Dhimi,<sup>a</sup> Li Li,<sup>d</sup> Bin Kong,<sup>e</sup> Yixue Su,<sup>a</sup> Kevin A. Schug,<sup>d</sup> Jian Yang\*<sup>a</sup>

<sup>a</sup> Department of Biomedical Engineering, Materials Research Institutes, the Huck Institutes of Life Sciences, The Pennsylvania State University, University Park, PA 16801

<sup>b</sup> Beijing Laboratory of Biomedical Materials, Beijing University of Chemical Technology, Beijing China 100029

<sup>c</sup> Institute of Medical Engineering and Science, Massachusetts Institute of Technology, Cambridge, MA 02139

<sup>d</sup> Department of Chemistry and Biochemistry, University of Texas at Arlington, Arlington, TX 76010

<sup>e</sup> Institute of Chemistry, Chinese Academy of Sciences, Beijing, China 100190

\* To whom correspondence should be addressed. Email: [jxy30@psu.edu](mailto:jxy30@psu.edu)

**Identification of examples of CPDs:**

CA-Cys:  $^1\text{H}$  NMR (DMSO- $d_6$ )  $\delta$  6.58 (d, 1H), 5.48 (d, 1H), 3.90 (t, 1H), 3.60 (d, 2H).  $^{13}\text{C}$  NMR (DMSO- $d_6$ )  $\delta$  169.7, 166.1, 161.5, 150.4, 143.2, 115.5, 98.7, 63.0, 32.2. ESI-MS  $m/z=241$ :  $(\text{M}+\text{H})^+$ ;  $m/z=264$ :  $(\text{M}+\text{Na})^+$ .

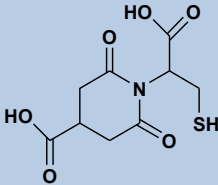
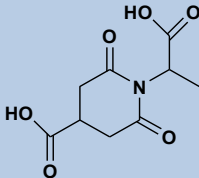
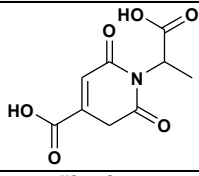
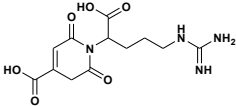
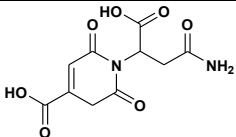
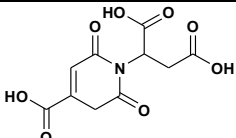
CA-Cysteamine:  $^1\text{H}$  NMR (DMSO- $d_6$ )  $\delta$  6.54 (d, 1H), 4.37 (t, 1H), 3.53 (t, 2H), 2.51-3.12 (m, 2H).  $^{13}\text{C}$  NMR (DMSO- $d_6$ )  $\delta$  171.5, 160.6, 148.7, 101.3, 84.7, 57.5, 49.9, 34.0. ESI-MS  $m/z=198$ :  $(\text{M}+\text{H})^+$ .

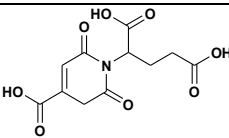
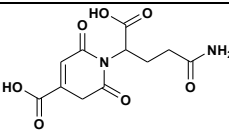
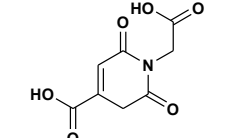
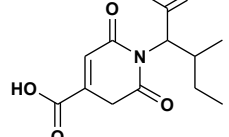
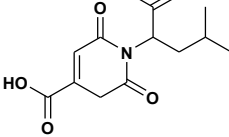
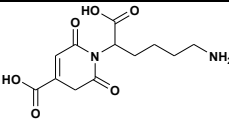
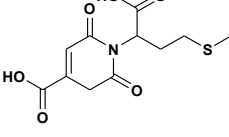
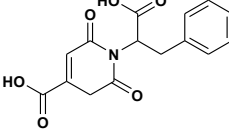
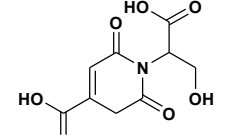
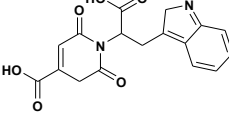
CA-Propylamine:  $^1\text{H}$  NMR (DMSO- $d_6$ )  $\delta$  6.18-6.49 (s, 1H), 3.32-3.37 (t, 2H), 2.76-3.01 (m, 2H), 1.45-1.52 (q, 2H), 0.80-0.85 (t, 3H).  $^{13}\text{C}$  NMR (DMSO- $d_6$ )  $\delta$  179.5, 175.9, 172.3, 166.9, 141.9, 42.74, 40.0, 22.2, 11.9. ESI-MS  $m/z=216$ :  $(\text{M}+\text{H}_2\text{O}+\text{H})^+$ ;  $m/z=238$ :  $(\text{M}+\text{H}_2\text{O}+\text{Na})^+$ .

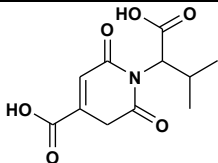
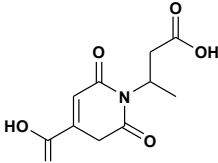
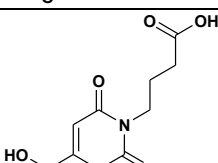
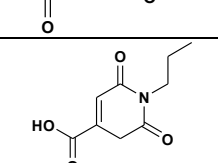
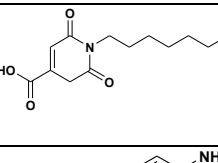
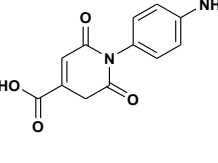
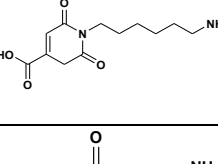
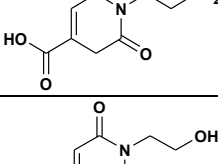
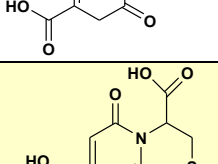
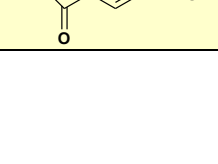
CA-Ala:  $^1\text{H}$  NMR (DMSO- $d_6$ )  $\delta$  4.58-4.78 (m, 1H), 2.50-3.07 (m, 4H), 1.32 (d, 3H).  $^{13}\text{C}$  NMR (DMSO- $d_6$ )  $\delta$  178.6, 174.8, 172.1, 171.5, 72.3, 47.7, 39.7, 14.5. ESI-MS  $m/z=228$ :  $(\text{M}+\text{H})^+$ ;  $m/z=268$ :  $(\text{M}+\text{H}_2\text{O}+\text{Na})^+$ .

CA-Gly:  $^1\text{H}$  NMR (DMSO- $d_6$ )  $\delta$  6.58 (s, 1H), 4.08-4.21 (m, 2H), 2.50-2.89 (m, 2H).  $^{13}\text{C}$  NMR (DMSO- $d_6$ )  $\delta$  175.3, 172.0, 169.0, 166.7, 140.9, 72.8, 39.8, 34.9. ESI-MS  $m/z=232$ :  $(\text{M}+\text{H}_2\text{O}+\text{H})^+$ ;  $m/z=254$ :  $(\text{M}+\text{H}_2\text{O}+\text{Na})^+$ ;  $m/z=311$ :  $(\text{M}+\text{Gly}+\text{H}_2\text{O}+\text{Na})^+$ .

**Table S1.** Summary of synthesis and photophysical properties of CPDs. Compound 1 is the aliphatic acid, compound 2 is one of the listed primary amines, amino acids, or analogs of amino acids.  $\lambda_{ab}$  is the maximum absorption wavelength.  $\epsilon$  is the extinction coefficient.  $\lambda_{ex}$  and  $\lambda_{em}$  are the maximum excitation and emission wavelengths.  $\Phi$  is the quantum yield.

Compound 1	Compound 2	Fluorophore Structure	$\lambda_{ex}$ (nm)	$\lambda_{em}$ (nm)	$\epsilon$ ( $M^{-1}cm^{-1}$ )	$\Phi$ (%)	Stokes Shift (nm)	Band Shift ?
TCA	Cysteine		366	431	11.6	54.2	65	Y
TCA	Alanine		355	423	6.1	0.2	68	Y
SucA	Cysteine	NA	NA	NA	NA	0	NA	NA
SucA	Alanine	NA	NA	NA	NA	0	NA	NA
CA	Propionic acid	NA	NA	NA	NA	0	NA	NA
CA	3-mercaptopropionic acid	NA	NA	NA	NA	0	NA	NA
CA	Alanine		361	430	79	21.2	69	Y
CA	Arginine		382	451	11.6	15.5	69	Y
CA	Asparagine		378	440	35.5	23.8	62	Y
CA	Aspartic Acid		356	427	6.8	19.7	71	Y

CA	Glutamic Acid		358	423	5.1	9.1	65	Y
CA	Glutamine		383	448	102.4	7.3	65	Y
CA	Glycine		357	434	12	39.0	77	Y
CA	Isoleucine		357	430	5.6	17.2	73	Y
CA	Leucine		359	423	6.2	8.8	64	Y
CA	Lysine		359	431	11.4	8.6	72	Y
CA	Methionine		362	424	5.3	10.5	62	Y
CA	Phenylalanine		358	423	7.8	12.7	65	Y
CA	Serine		369	440	437.9	4.2	71	Y
CA	Tryptophan		386	445	14.6	5	59	Y

CA	Valine		361	428	5.3	17.5	67	Y
CA	3-Aminobutanoic Acid		356	430	6.3	8.8	74	Y
CA	$\gamma$ -Aminobutyric acid		355	422	4.9	22.1	67	Y
CA	Propylamine		359	424	6.6	24.6	65	Y
CA	Heptylamine		356	424	4.7	13.5	68	Y
CA	Phenylenediamine		360	433	12.1	4.5	73	Y
CA	Hexamethylenediamine		357	426	9.4	11.5	69	Y
CA	ethylenediamine		377	440	828.3	9.2	63	Y
CA	ethanolamine		368	419	34.6	42.1	51	Y
CA	Cysteine		364	445	8640	81.4	81	N

CA	Cysteamine		365	445	3880	79 .3	80	N
CA	Homocysteine		375	445	1014	70 .8	70	N
CA	Threonine		386	436	418	78 .6	50	N
CA	2-Aminothiophenol		396	439	877.8	98 .5	43	N
CA	Penicillamine		369	432	3180	80 .6	63	N

**Table S2.** Harmonic Oscillator Model of Electron Delocalization (HOMED) and Nucleus Independent Chemical Shift (NICS) values of selected citric acid based dyes. CA-Cys, CA-Homocysteine, CA-Cysteamine are examples for TPAs. CA-Ala, CA-Gly, and CA-Propylamine are examples for DPRs.

	CA-Cys	CA-HomoCys	CA-Cysteamine	CA-Ala	CA-Gly	CA-Propylamine
NICS	-3.2671	-3.0824	-3.0674	1.5852	1.7880	1.8341

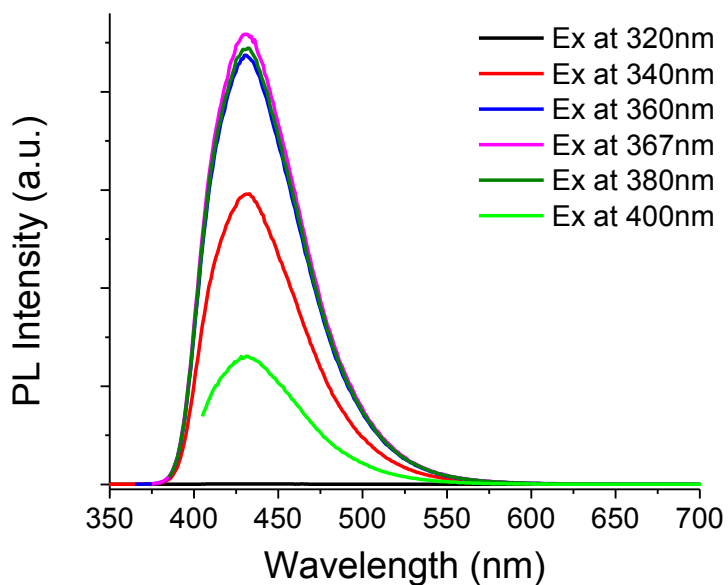


**Figure S1.** Emission spectra of CA-Cysteamine under different excitation wavelengths.

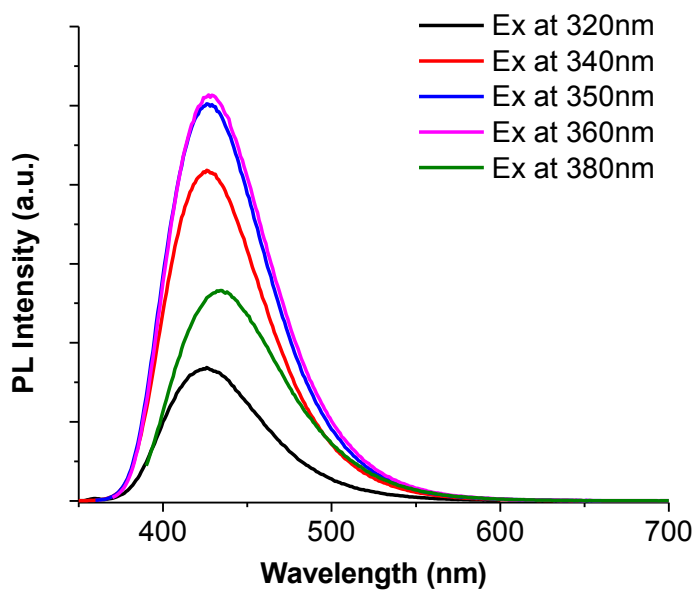


**Figure S2.** Emission spectra of CA-Homocysteine under different excitation wavelengths.

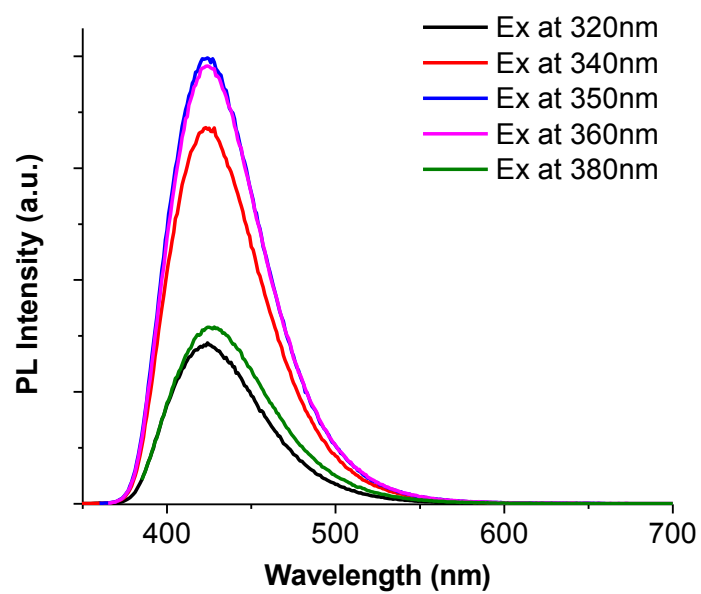


**Figure S3.** Emission spectra of CA-Penicillamine under different excitation wavelengths.

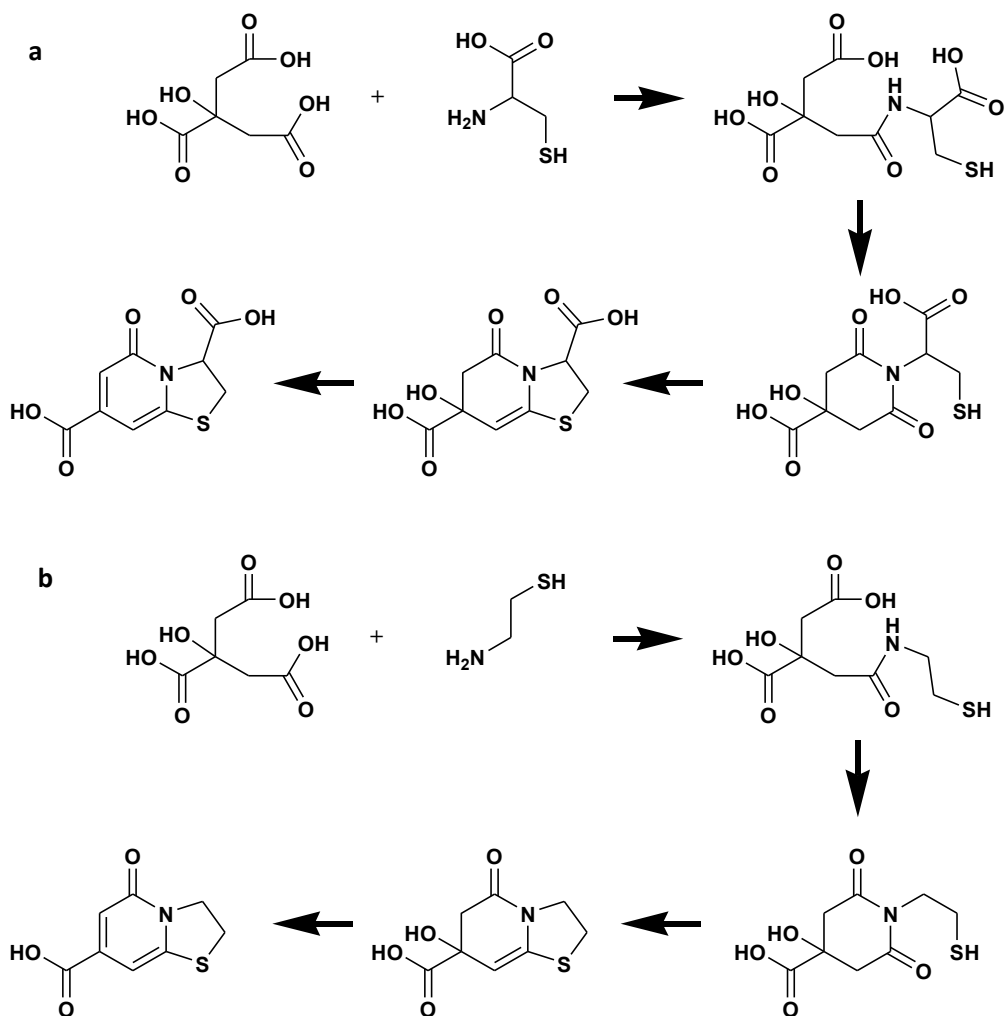


**Figure S4.** Scheme of proposed reaction steps between citric acid and (a) cysteine or (b) cysteamine to form CA-Cys or CA-Cysteamine dyes.

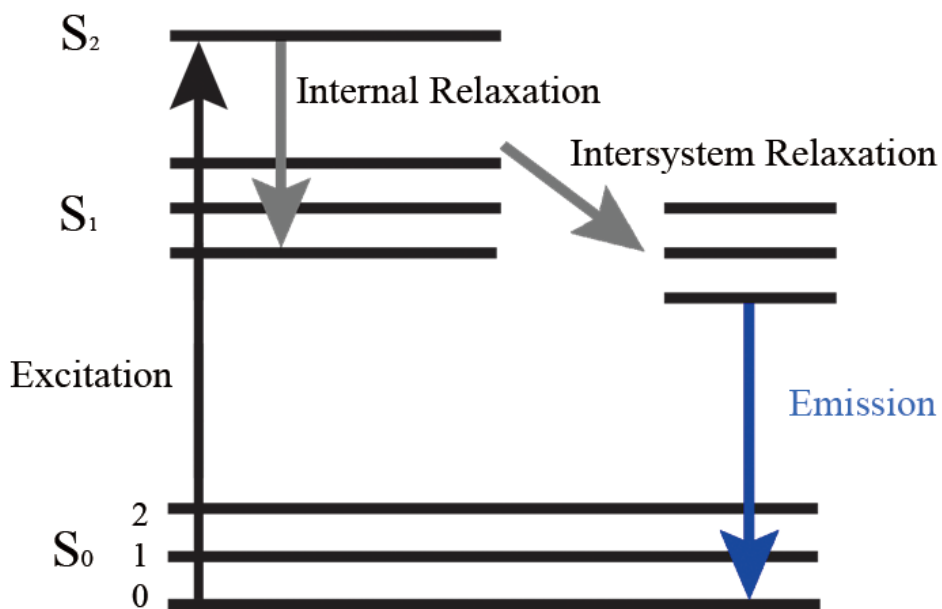


**Figure S5.** A Jablonski diagram of fluorescence excitation and emission processes of a TPA fluorophore.

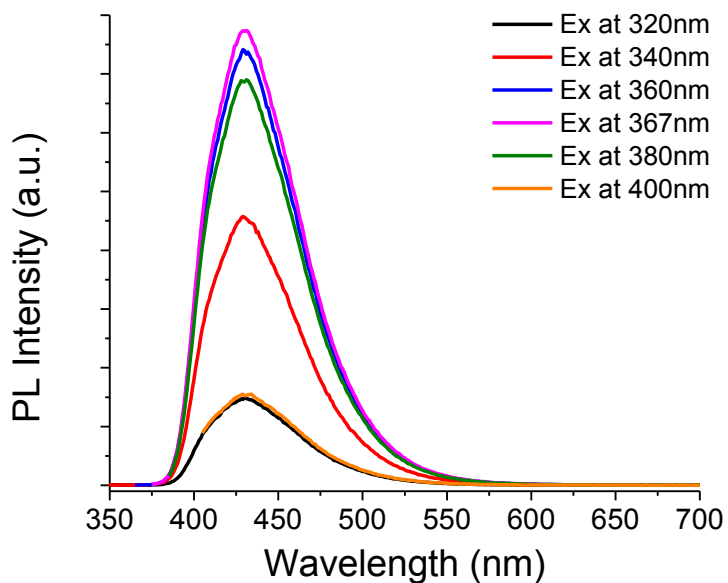


**Figure S6.** Emission spectra of BPLP-TPA under different excitation wavelengths.

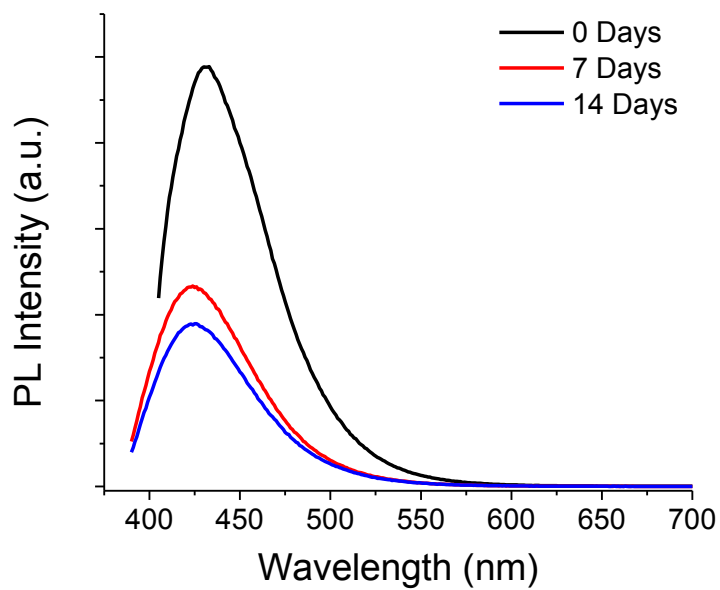


**Figure S7.** Emission spectra of BPLP-Cys degradation products in 1M NaOH solution.

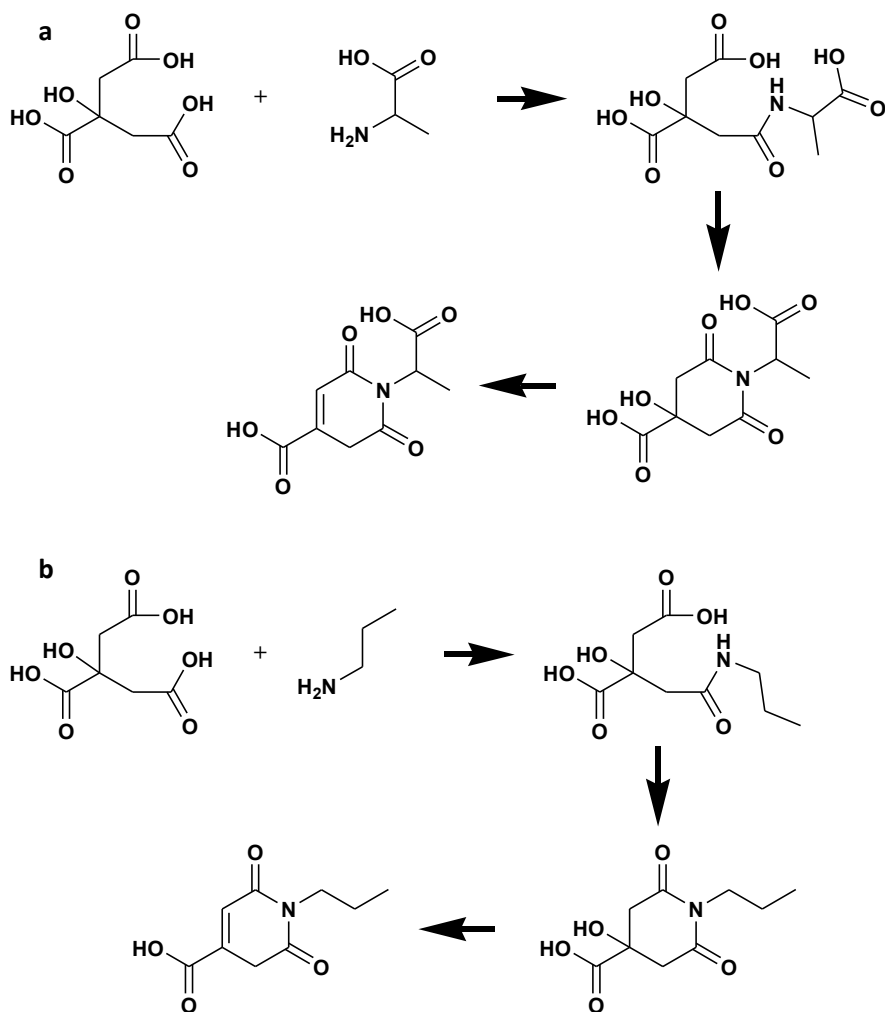


**Figure S8.** Scheme of proposed reaction steps between citric acid and (a) alanine or (b) propylamine to form DPR dyes.

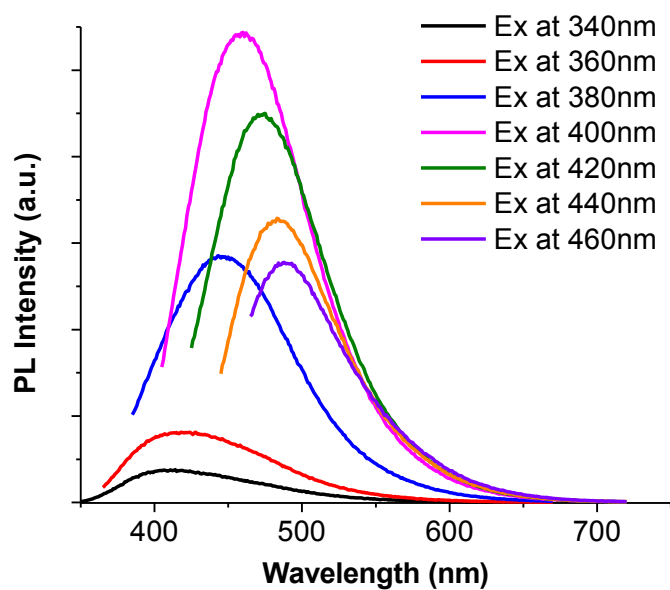


**Figure S9.** Emission spectra of CA-Gly at different excitation wavelengths.

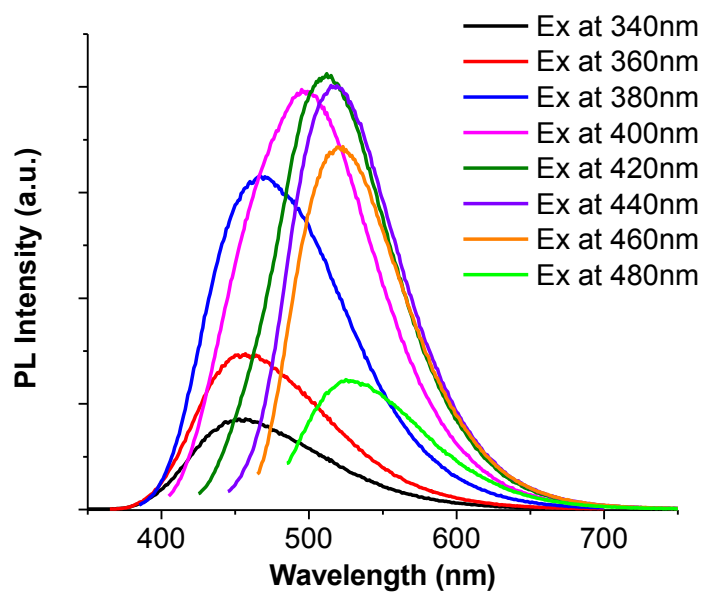


**Figure S10.** Emission spectra of CA-Propylamine at different excitation wavelengths.

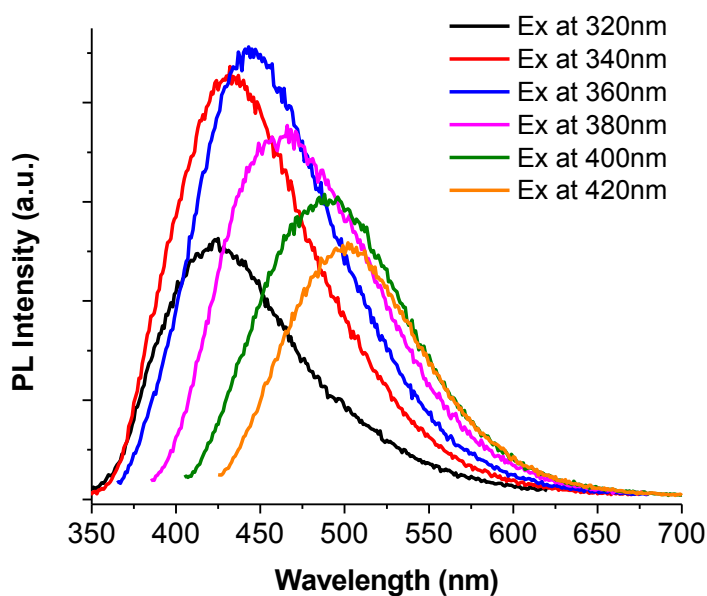


**Figure S11.** Emission spectra of BPLP-Ala degradation products in 1M NaOH solution

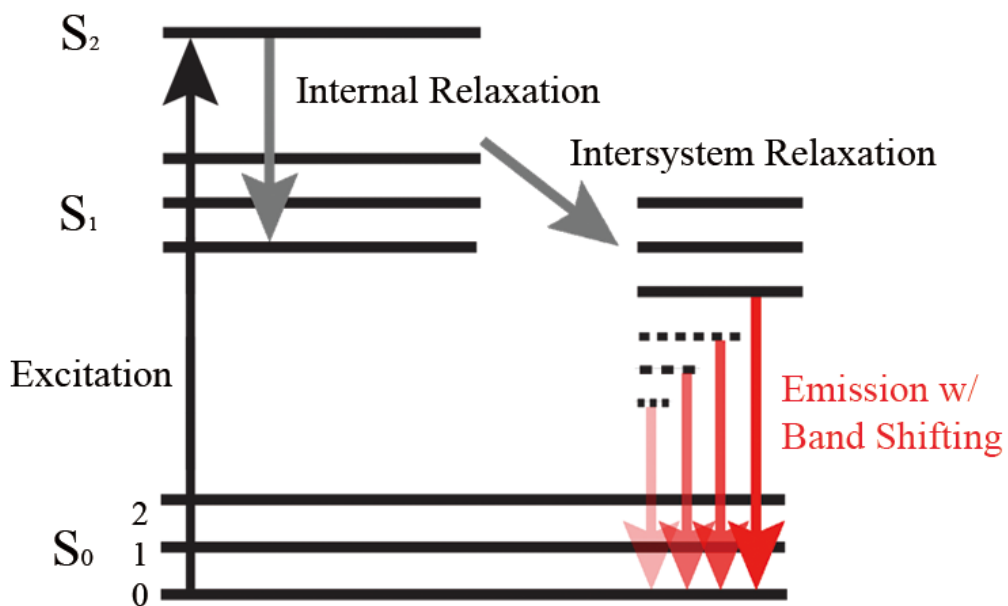


**Figure S12.** A Jablonski diagram of fluorescence excitation and emission processes showing band shifting behaviors of a DPR fluorophore.

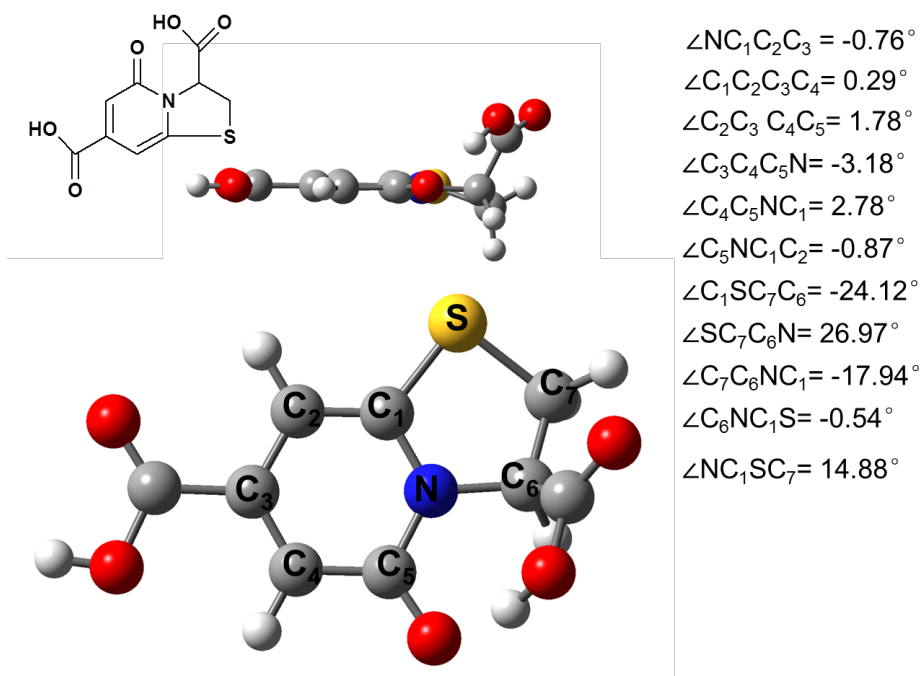


**Figure S13.** Spatial conformations of CA-Cys. Dihedral angles of any four atoms are listed on the right side.

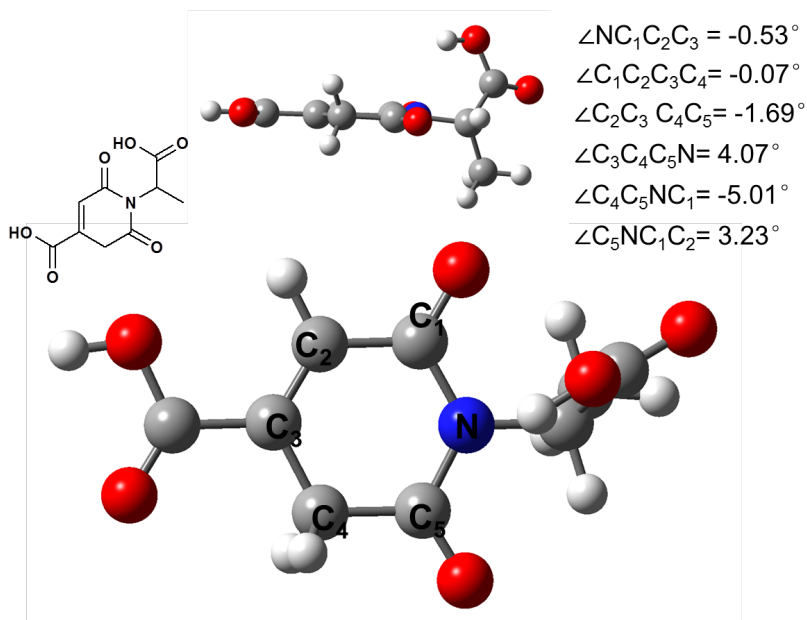


**Figure S14.** Spatial conformations of CA-Ala. Dihedral angles of any four atoms are listed on the right side.

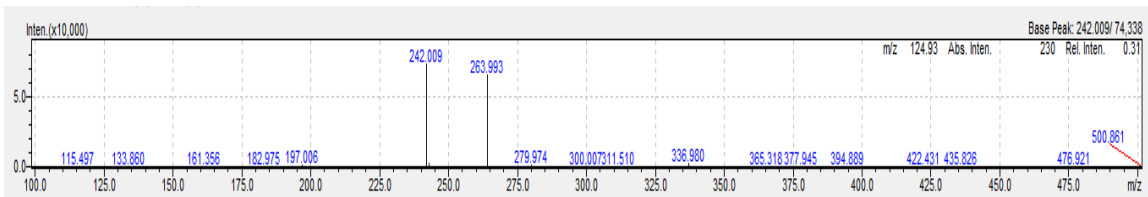


**Figure S15.** ESI-MS spectrum (m/z) of CA-Cys. m/z=241: (M+H)<sup>+</sup>; m/z=264: (M+Na)<sup>+</sup>.

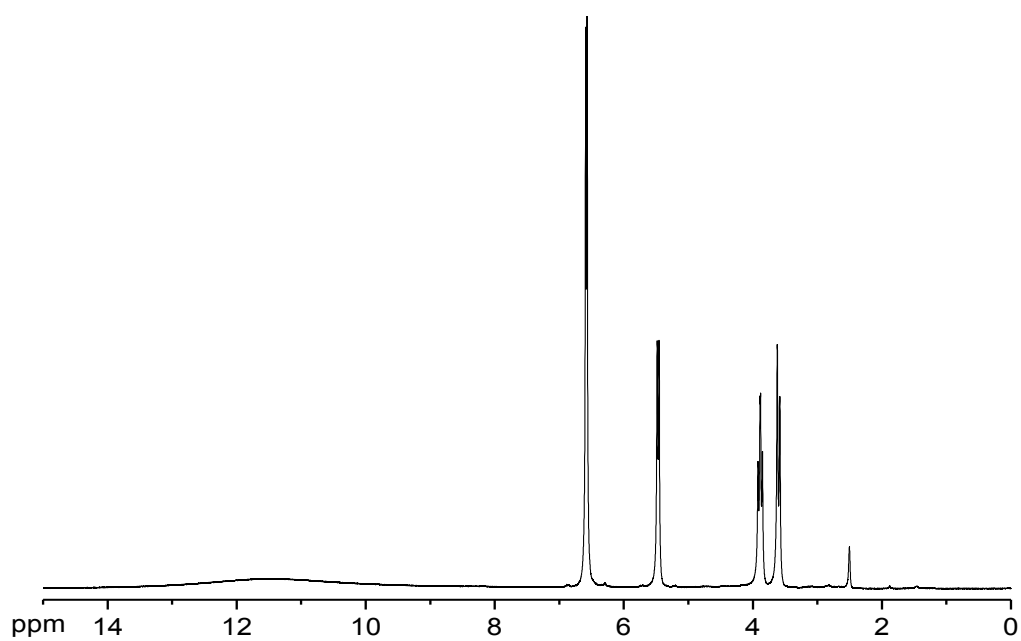


**Figure S16.** <sup>1</sup>H NMR (DMSO-d<sub>6</sub>) spectrum of CA-Cys. δ 6.58 (d, 1H), 5.48 (d, 1H), 3.90 (t, 1H), 3.60 (d, 2H).

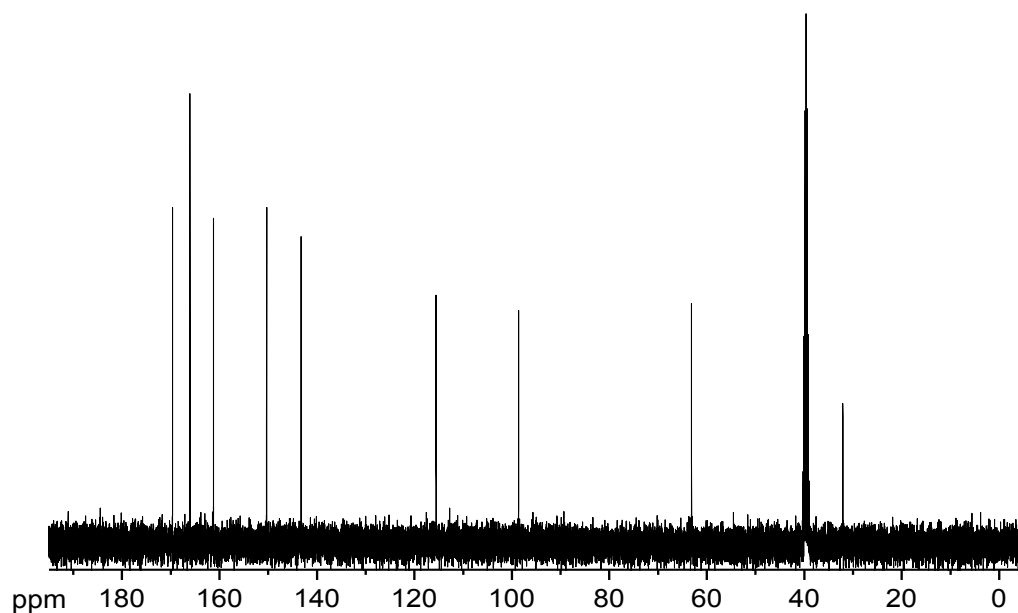


**Figure S17.**  $^{13}\text{C}$  NMR (DMSO- $d_6$ ) spectrum of CA-Cys.  $\delta$  169.7, 166.1, 161.5, 150.4, 143.2, 115.5, 98.7, 63.0, 32.2.

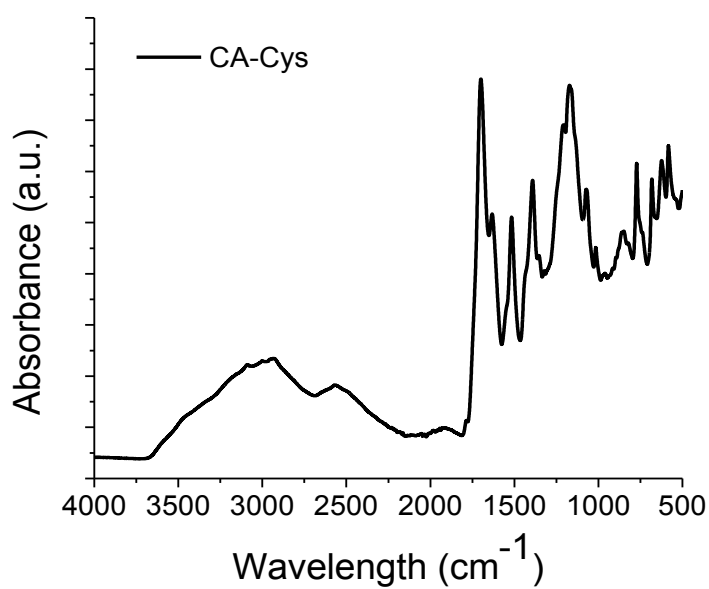


**Figure S18.** FT-IR spectrum of CA-Cys.

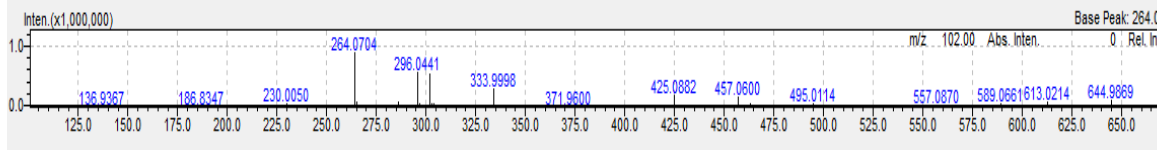


**Figure S19.** ESI-MS spectrum (m/z) of BPLP-Cys degradation product. m/z=264: (M+Na)<sup>+</sup>.

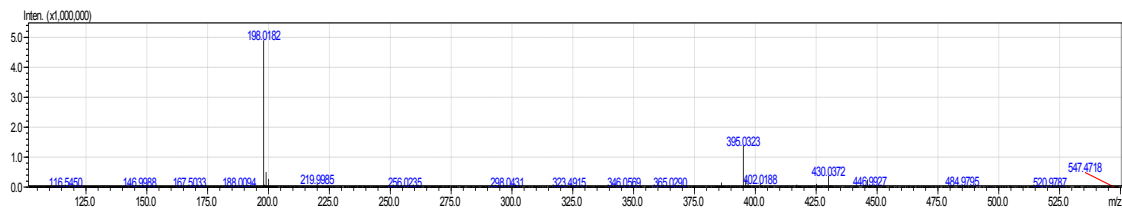


**Figure S20.** ESI-MS spectrum (m/z) of CA-Cysteamine. m/z= 198: (M+H)<sup>+</sup>.

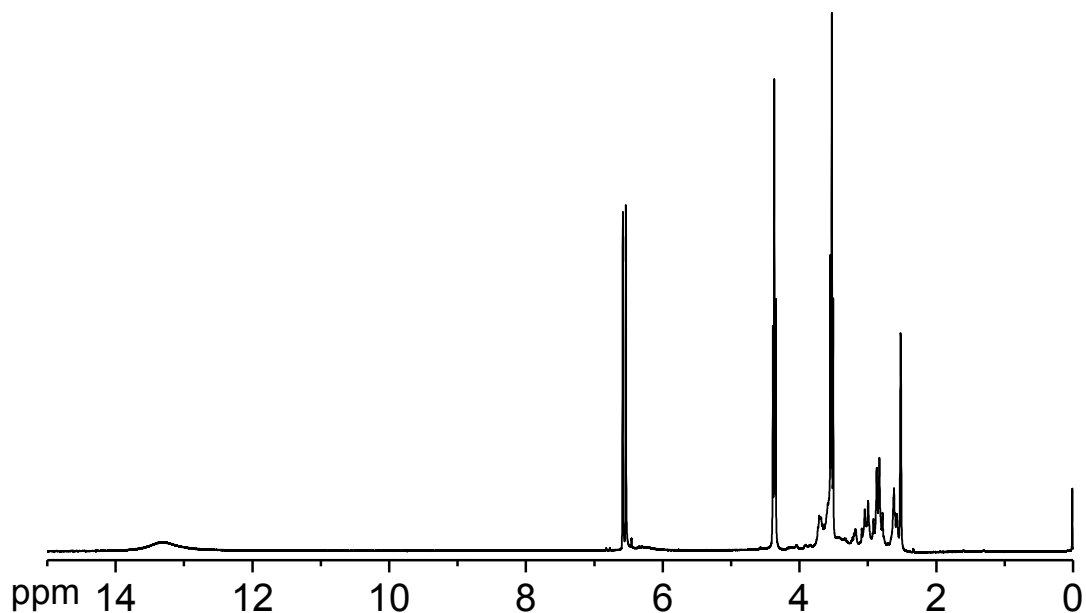


**Figure S21.** <sup>1</sup>H NMR (DMSO-d<sub>6</sub>) spectrum of CA-Cysteamine. δ 6.54 (d, 1H), 4.37 (t, 1H), 3.53 (t, 2H), 2.51-3.12 (m, 2H).

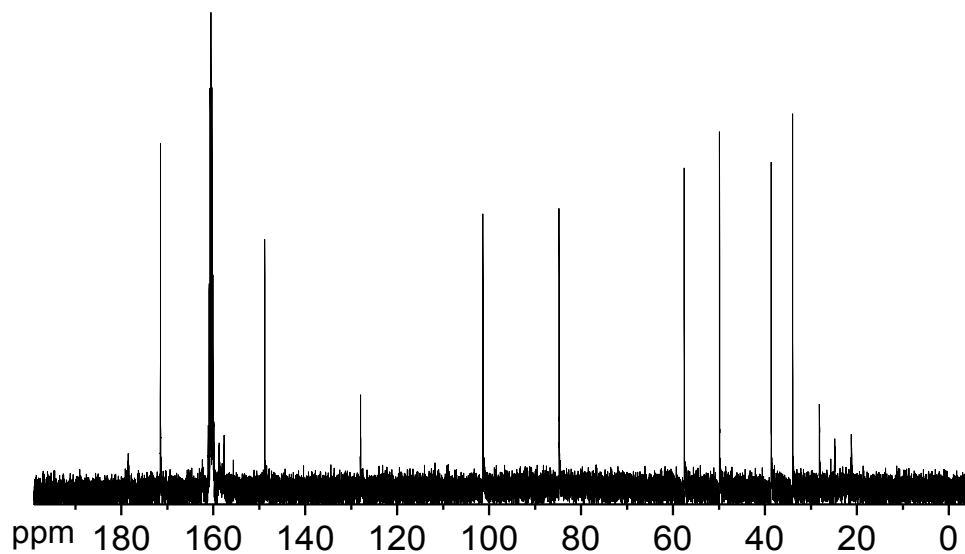


**Figure S22.**  $^{13}\text{C}$  NMR (DMSO- $d_6$ ) spectrum of CA-Cysteamine.  $\delta$  171.5, 160.6, 148.7, 101.3, 84.7, 57.5, 49.9, 34.0.

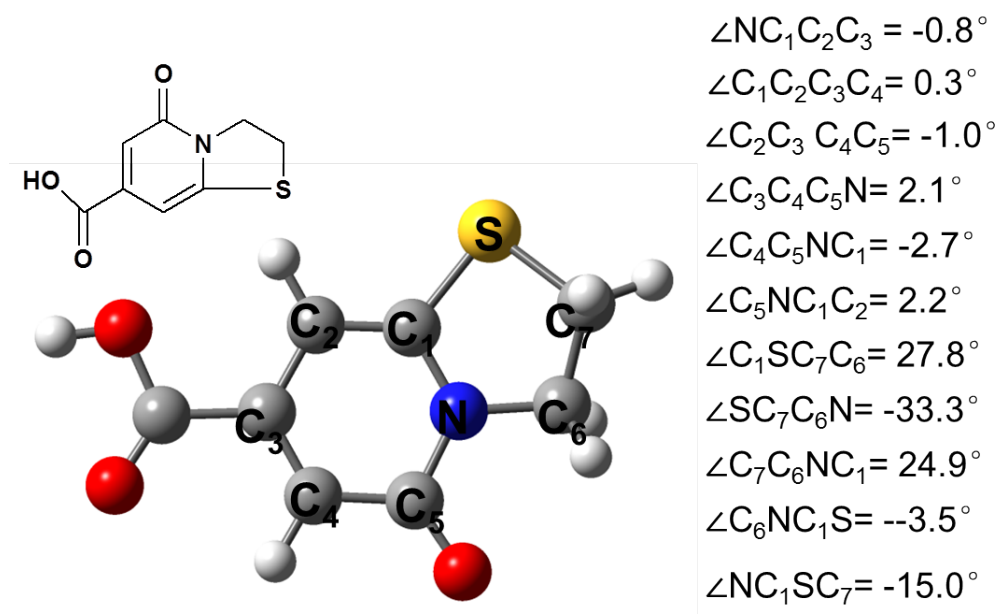


**Figure S23.** Spatial conformation of CA-Cysteamine. Dihedral angles of any four atoms are listed on the right side.

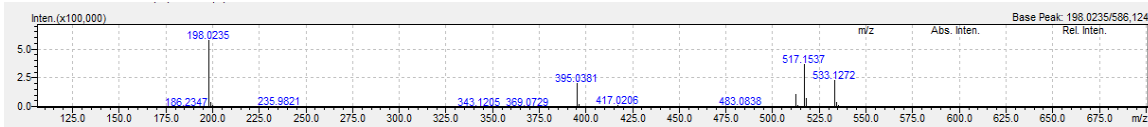


**Figure S24.** ESI-MS spectrum ( $m/z$ ) of BPLP-Cysteamine degradation product.  $m/z=198$ :  $(M+H)^+$ .

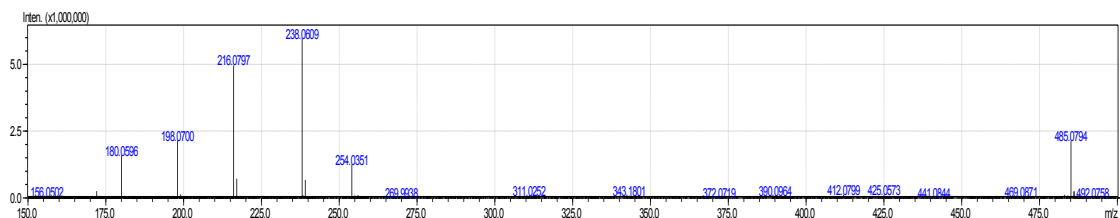


**Figure S25.** ESI-MS spectrum ( $m/z$ ) of CA-Propylamine.  $m/z=216$ :  $(M+H_2O+H)^+$ ;  
 $m/z=238$ :  $(M+H_2O+Na)^+$ .

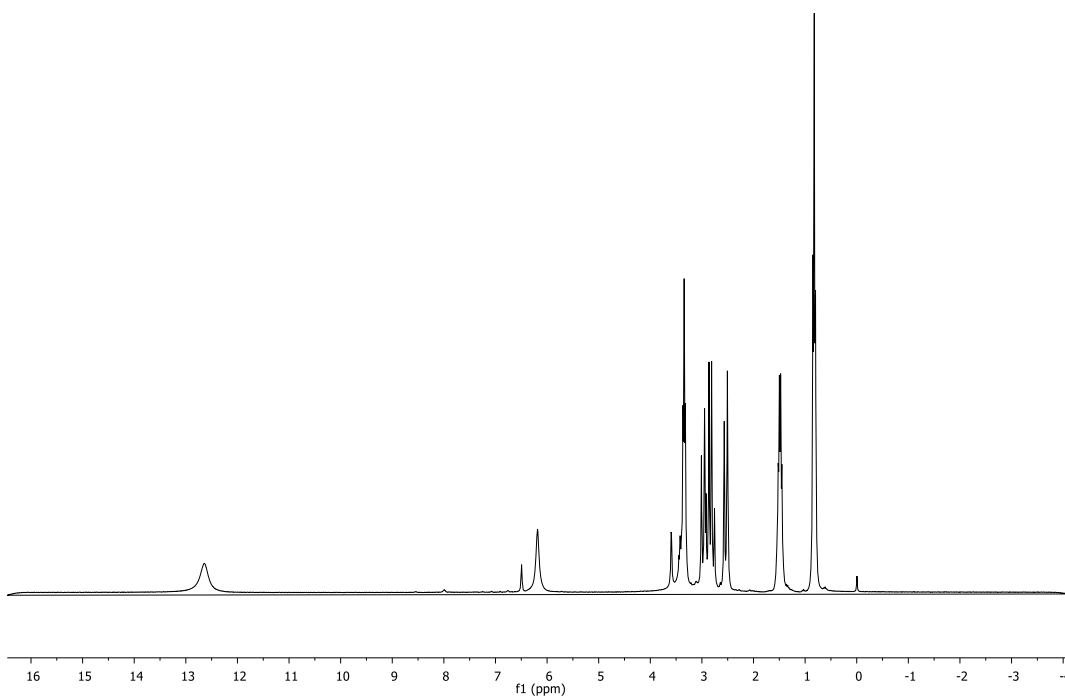


**Figure S26.**  $^1H$  NMR ( $DMSO-d_6$ ) spectrum of CA-Propylamine.  $\delta$  6.18-6.49 (s, 1H),  
 3.32-3.37 (t, 2H), 2.76-3.01 (m, 2H), 1.45-1.52 (q, 2H), 0.80-0.85 (t, 3H).

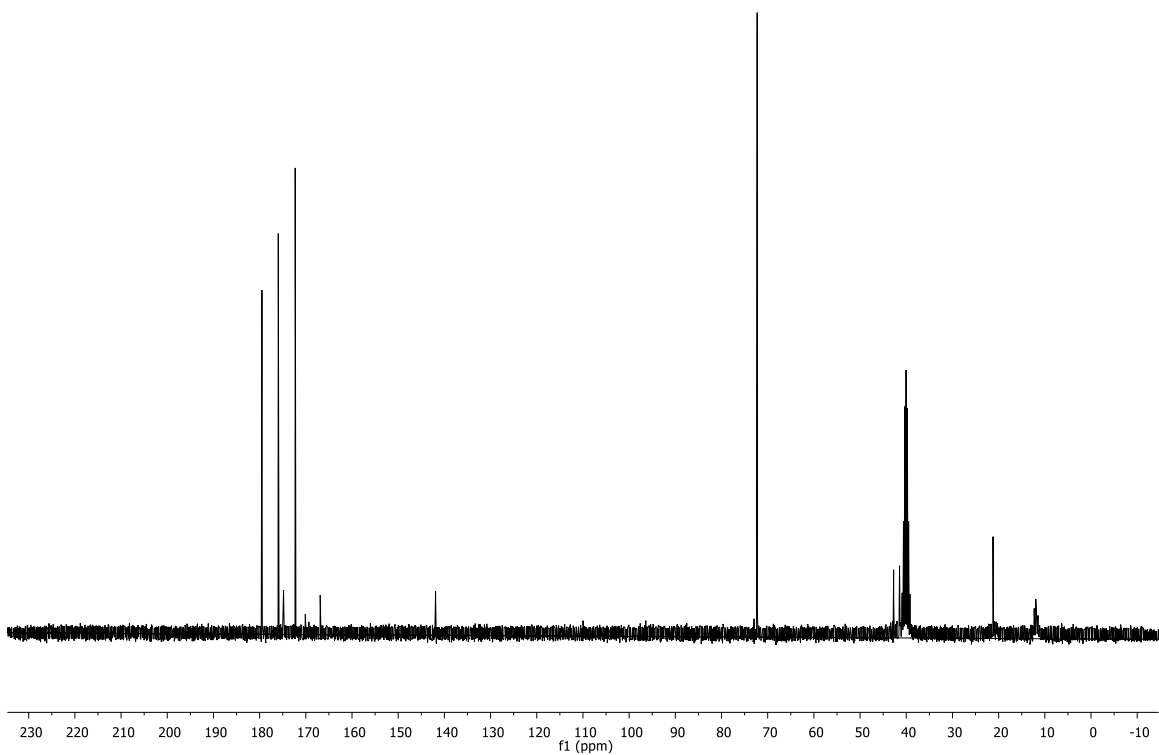


**Figure S27.**  $^{13}\text{C}$  NMR (DMSO- $d_6$ ) spectrum of CA-Propylamine.  $\delta$  179.5, 175.9, 172.3, 166.9, 141.9, 42.74, 40.0, 22.2, 11.9.

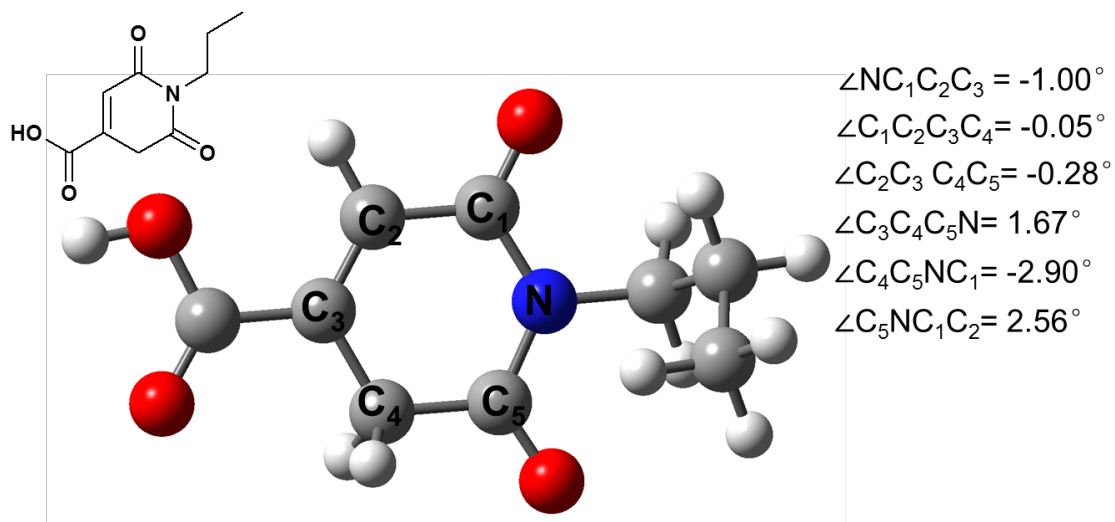


**Figure S28.** Spatial conformation of CA-Propylamine. Dihedral angles of any four atoms are listed on the right side.

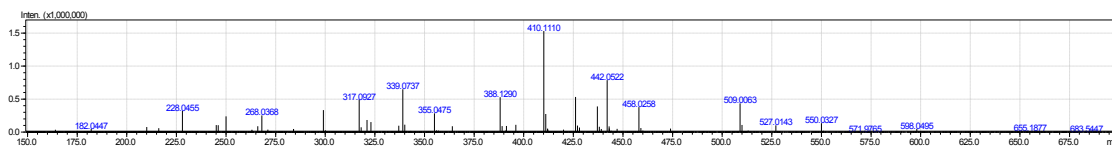


**Figure S29.** ESI-MS spectrum (m/z) of CA-Ala. m/z=228: (M+H)<sup>+</sup>; m/z=268: (M+H<sub>2</sub>O+Na)<sup>+</sup>.

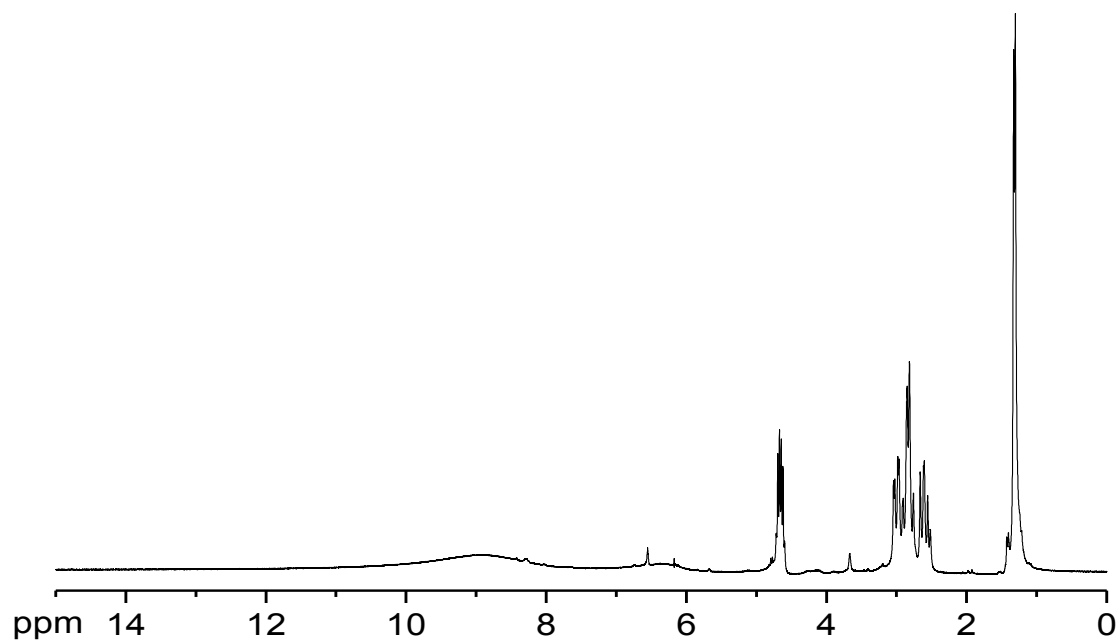


**Figure S30.** <sup>1</sup>H NMR (DMSO-d<sub>6</sub>) spectrum of CA-Ala. δ 4.58-4.78 (m, 1H), 2.50-3.07 (m, 4H), 1.32 (d, 3H).

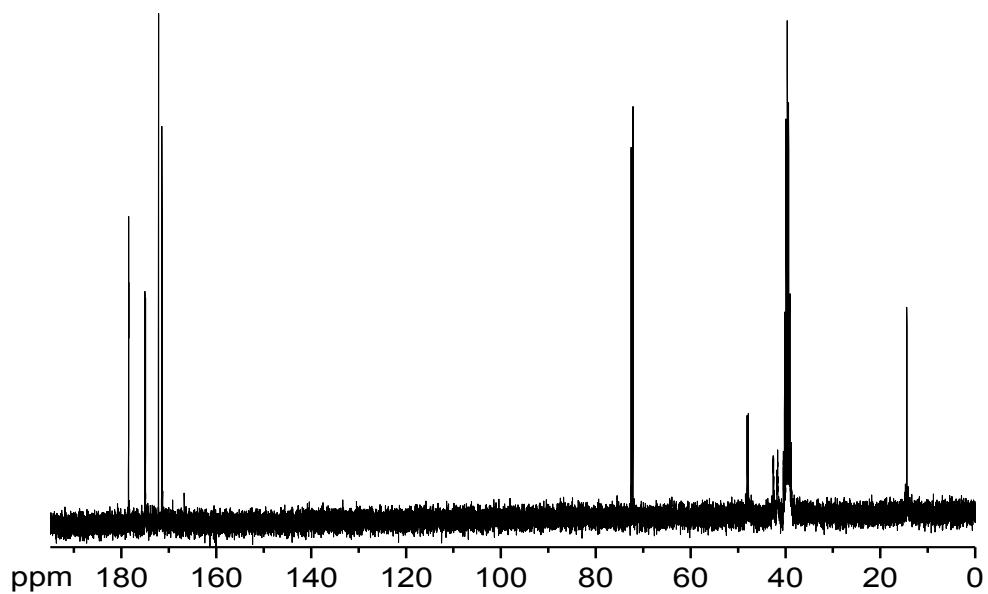


**Figure S31.**  $^{13}\text{C}$  NMR (DMSO- $d_6$ ) spectrum of CA-Ala.  $\delta$  178.6, 174.8, 172.1, 171.5, 72.3, 47.7, 39.7, 14.5.

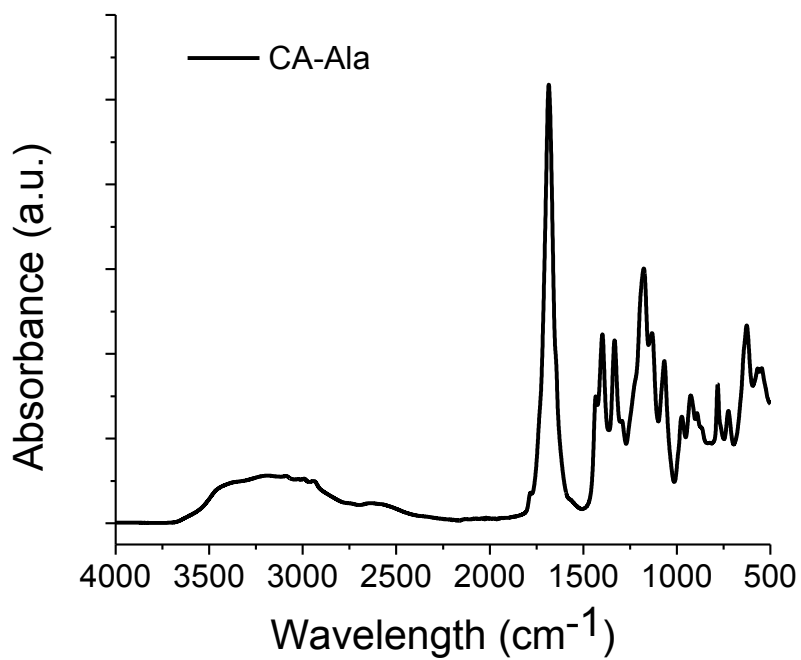


**Figure S32.** FT-IR spectrum of CA-Ala.

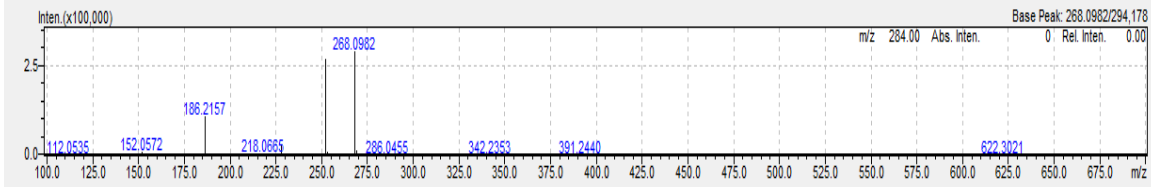


**Figure S33.** ESI-MS spectrum (m/z) of BPLP-Ala degradation product. m/z=250: (M+Na)<sup>+</sup>, m/z=268: (M+H<sub>2</sub>O+Na)<sup>+</sup>.

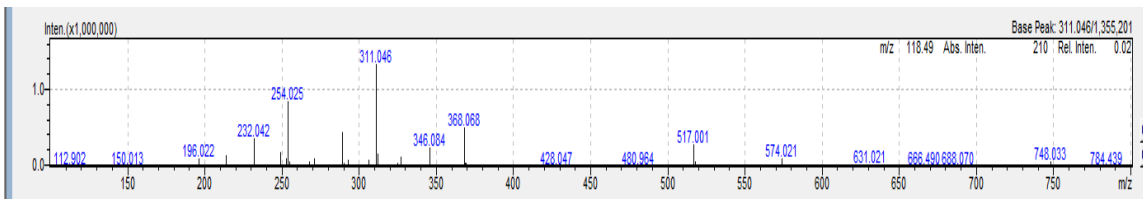


**Figure S34.** ESI-MS spectrum (m/z) of CA-Gly. m/z=232: (M+H<sub>2</sub>O+H)<sup>+</sup>; m/z=254: (M+H<sub>2</sub>O+Na)<sup>+</sup>; m/z=311: (M+Gly+H<sub>2</sub>O+Na)<sup>+</sup>.

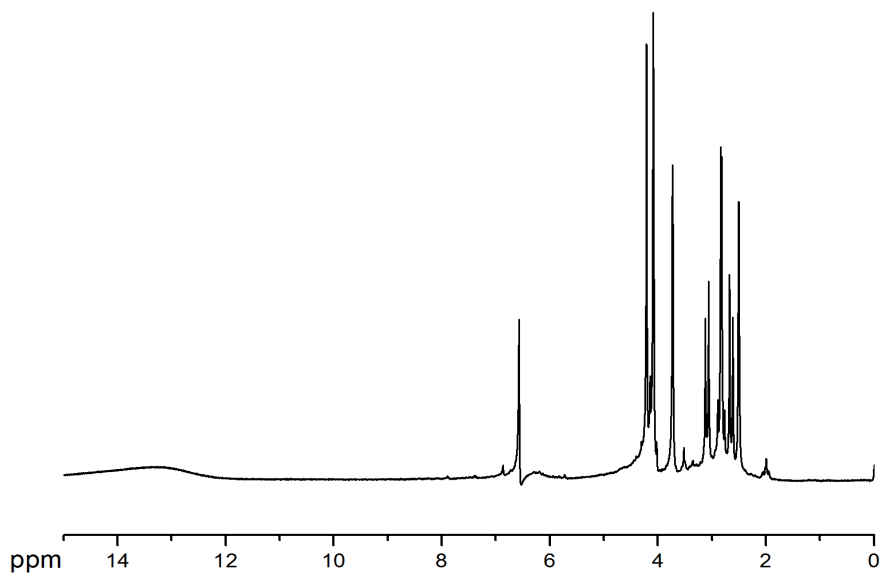


**Figure S35.** <sup>1</sup>H NMR spectrum of CA-Gly. δ 6.58 (s, 1H), 4.08-4.21 (m, 2H), 2.50-2.89 (m, 2H).

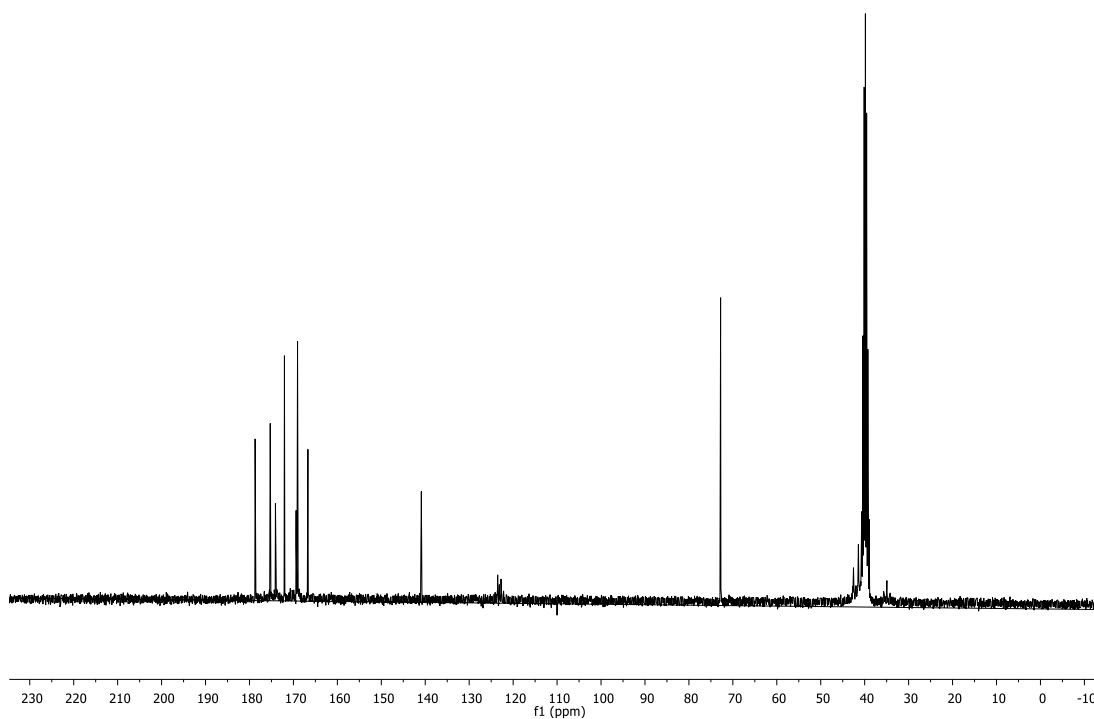


**Figure S36.**  $^{13}\text{C}$  NMR spectrum of CA-Gly.  $\delta$  175.3, 172.0, 169.0, 166.7, 140.9, 72.8, 39.8, 34.9.

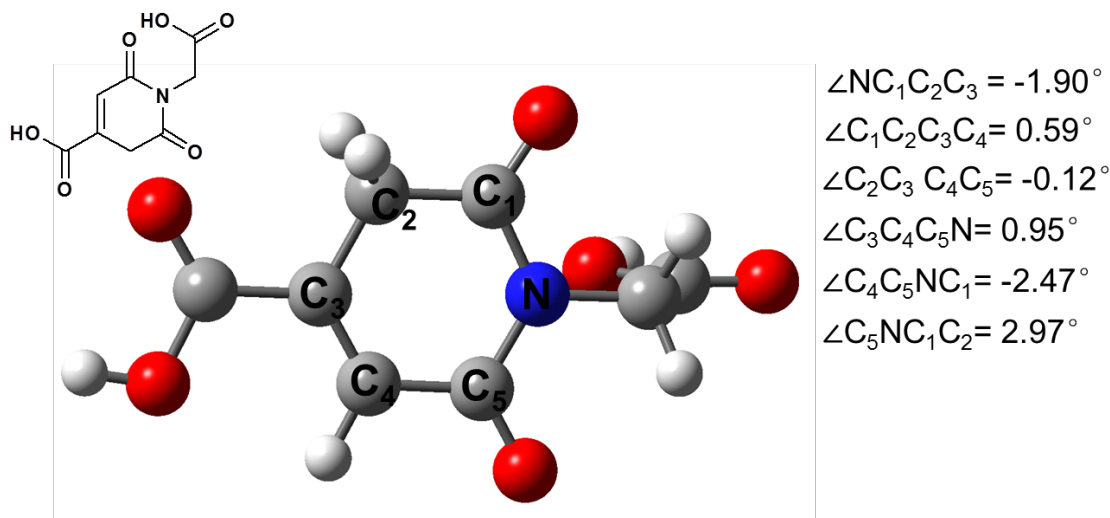


**Figure S37.** Spatial conformation of CA-Gly. Dihedral angles of any four atoms are listed on the right side.

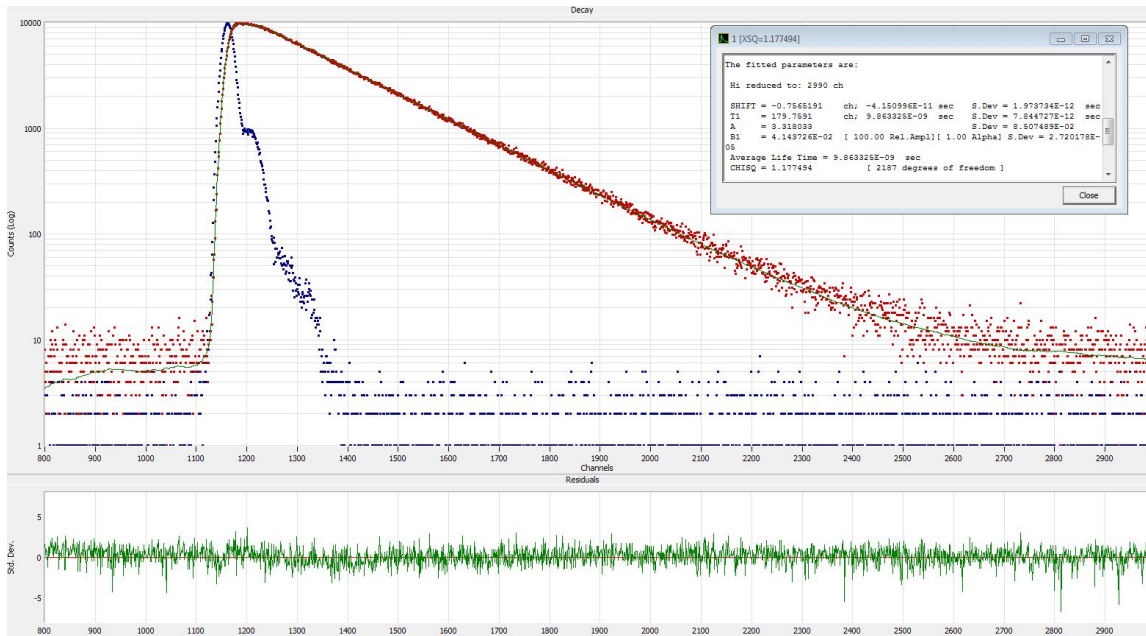


**Figure S38** Time-resolved fluorescence spectra of CA-Cys with a single exponential fitting (top), output lifetimes (inset), and the fitting residue distribution (bottom)

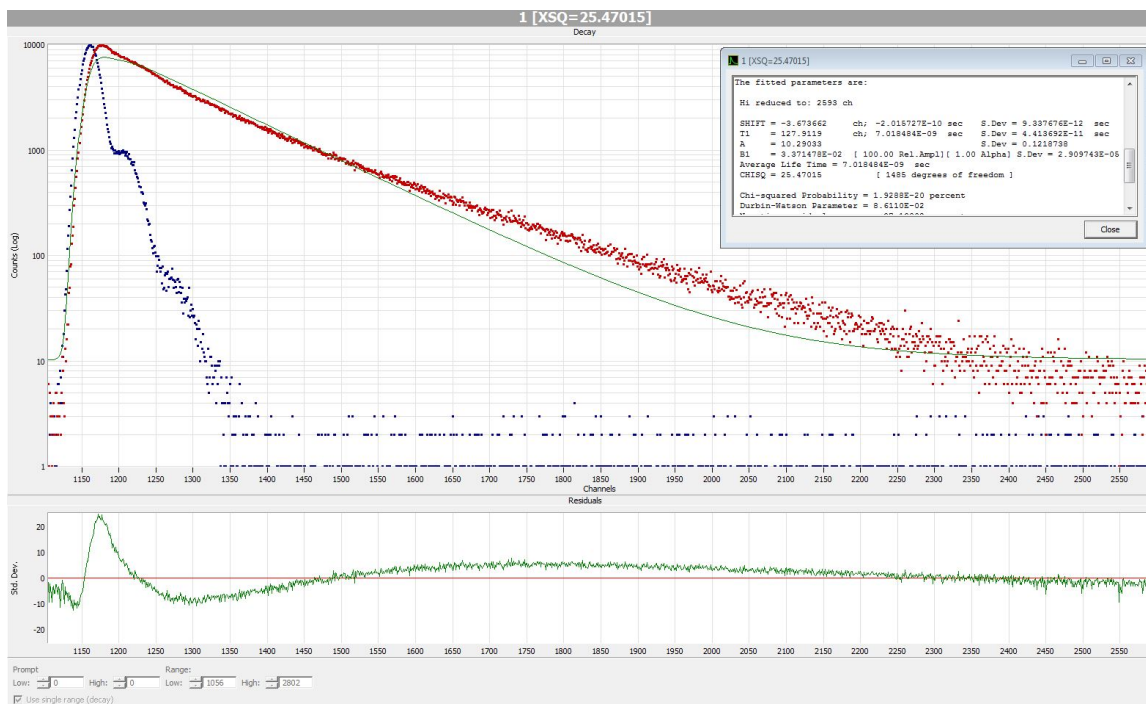


**Figure S39.** Time-resolved fluorescence spectra of CA-Ala with a single exponential fitting (top), output lifetimes (inset), and the fitting residue distribution (bottom)

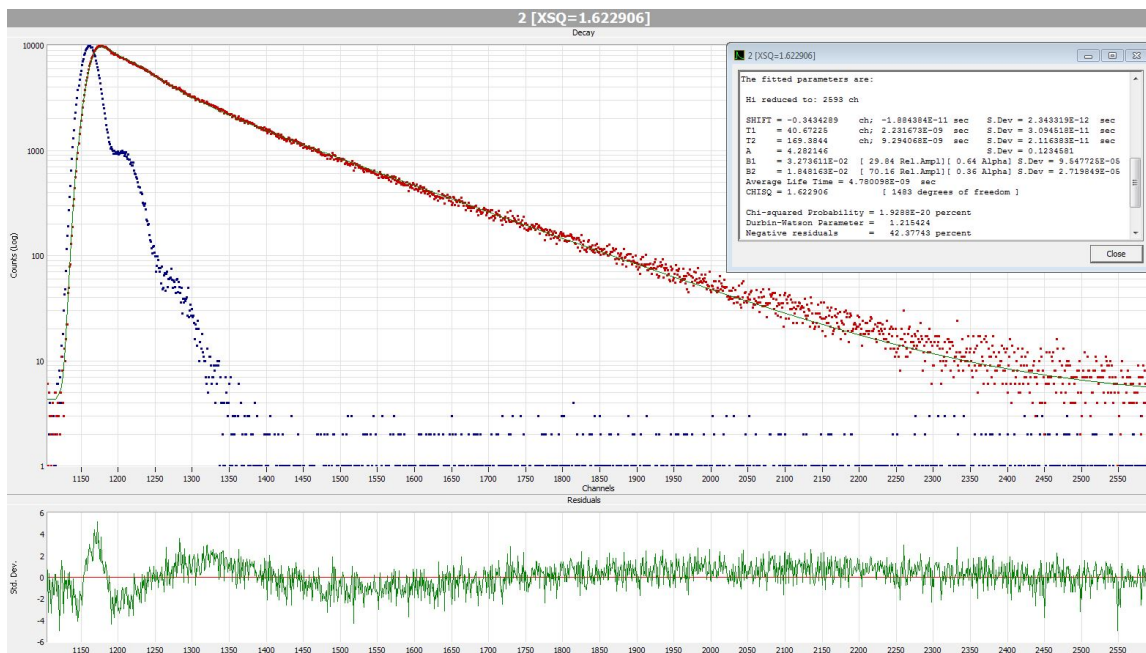


**Figure S40.** Time-resolved fluorescence spectra of CA-Ala with a double exponential fitting (top), output lifetimes (inset), and the fitting residue distribution (bottom)

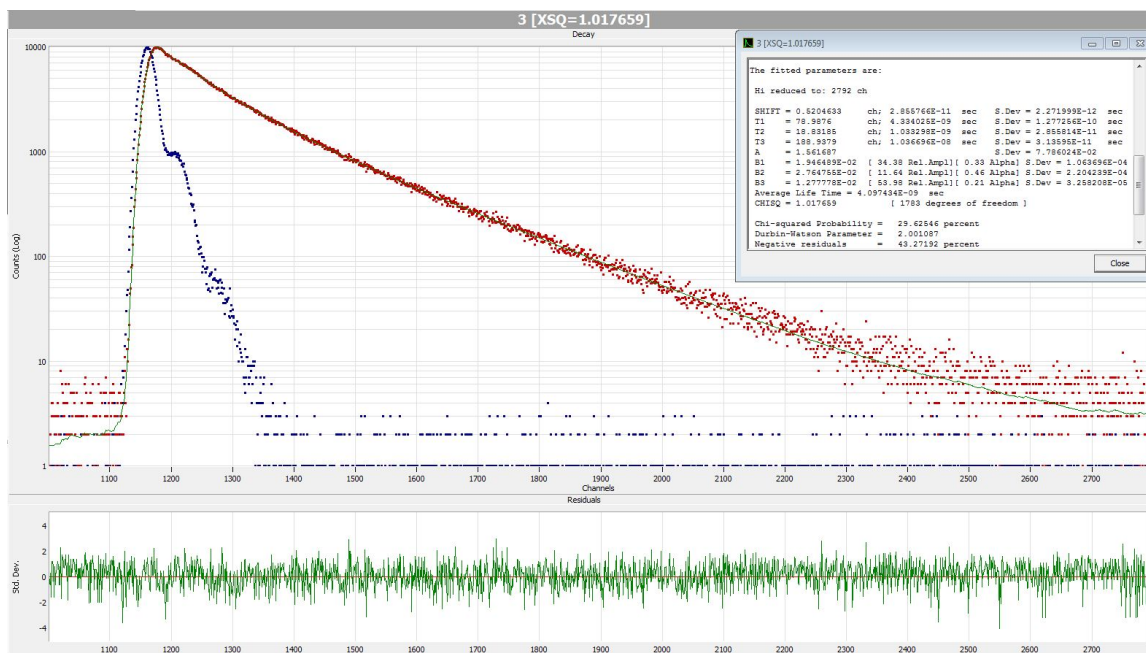


**Figure S41.** Time-resolved fluorescence spectra of CA-Ala with a triple exponential fitting (top), output lifetimes (inset), and the fitting residue distribution (bottom)

## REFERENCES

- [1] J. Yang, Y. Zhang, S. Gautam, L. Liu, J. Dey, W. Chen, R. P. Mason, C. A. Serrano, K. A. Schug, L. Tang, *Proceedings of the National Academy of Sciences of the United States of America* **2009**, *106*, 10086-10091.
- [2] M. J. Frisch, G. W. Trucks, H. B. Schlegel, G. E. Scuseria, M. A. Robb, J. R. Cheeseman, G. Scalmani, V. Barone, B. Mennucci, G. A. Petersson, H. Nakatsuji, M. Caricato, X. Li, H. P. Hratchian, A. F. Izmaylov, J. Bloino, G. Zheng, J. L. Sonnenberg, M. Hada, M. Ehara, K. Toyota, R. Fukuda, J. Hasegawa, M. Ishida, T. Nakajima, Y. Honda, O. Kitao, H. Nakai, T. Vreven, J. A. Montgomery Jr., J. E. Peralta, F. Ogliaro, M. J. Bearpark, J. Heyd, E. N. Brothers, K. N. Kudin, V. N. Staroverov, R. Kobayashi, J. Normand, K. Raghavachari, A. P. Rendell, J. C. Burant, S. S. Iyengar, J. Tomasi, M. Cossi, N. Rega, N. J. Millam, M. Klene, J. E. Knox, J. B. Cross, V. Bakken, C. Adamo, J. Jaramillo, R. Gomperts, R. E. Stratmann, O. Yazyev, A. J. Austin, R. Cammi, C. Pomelli, J. W. Ochterski, R. L. Martin, K. Morokuma, V. G. Zakrzewski, G. A. Voth, P. Salvador, J. J. Dannenberg, S. Dapprich, A. D. Daniels, Ö. Farkas, J. B. Foresman, J. V. Ortiz, J. Cioslowski, D. J. Fox, Gaussian, Inc., Wallingford, CT, USA, **2009**.
- [3] R. Krishnan, J. S. Binkley, R. Seeger, J. A. Pople, *The Journal of Chemical Physics* **1980**, *72*, 650-654.
- [4] R. Ditchfield, W. J. Hehre, J. A. Pople, *The Journal of Chemical Physics* **1971**, *54*, 724-728.
- [5] J. Kruszewski, T. M. Krygowski, *Tetrahedron Letters* **1972**, *13*, 3839-3842.
- [6] A. P. Demchenko, *Luminescence : the journal of biological and chemical luminescence* **2002**, *17*, 19-42.